OPEN ACCESS

Dynamically protected cat-qubits: a new paradigm for universal quantum computation

New Journal of Physics
The open access journal at the forefront of physics
Deutsche Physikalische Gesellschaft DPG | IOP Institute of Physics

Dynamically protected cat-qubits: a new paradigm for universal quantum computation

Mazyar Mirrahimi[1,2], Zaki Leghtas[2], Victor V Albert[2,3], Steven Touzard[2], Robert J Schoelkopf[2,3], Liang Jiang[2,3] and Michel H Devoret[2,3]

[1] INRIA Paris-Rocquencourt, Domaine de Voluceau, B.P. 105, F-78153 Le Chesnay Cedex, France
[2] Department of Applied Physics, Yale University, New Haven, Connecticut 06520, USA
[3] Department of Physics, Yale University, New Haven, Connecticut 06520, USA
E-mail: mazyar.mirrahimi@inria.fr

Received 6 December 2013, revised 24 February 2014
Accepted for publication 11 March 2014
Published 22 April 2014

New Journal of Physics **16** (2014) 045014

doi:10.1088/1367-2630/16/4/045014

Abstract

We present a new hardware-efficient paradigm for universal quantum computation which is based on encoding, protecting and manipulating quantum information in a quantum harmonic oscillator. This proposal exploits multi-photon driven dissipative processes to encode quantum information in logical bases composed of Schrödinger cat states. More precisely, we consider two schemes. In a first scheme, a two-photon driven dissipative process is used to stabilize a logical qubit basis of two-component Schrödinger cat states. While such a scheme ensures a protection of the logical qubit against the photon dephasing errors, the prominent error channel of single-photon loss induces bit-flip type errors that cannot be corrected. Therefore, we consider a second scheme based on a four-photon driven dissipative process which leads to the choice of four-component Schrödinger cat states as the logical qubit. Such a logical qubit can be protected against single-photon loss by continuous photon number parity measurements. Next, applying some specific Hamiltonians, we provide a set of universal quantum gates on the encoded qubits of each of the two schemes. In particular, we illustrate how these operations can be rendered fault-tolerant with respect to various decoherence channels of participating quantum systems. Finally, we also propose experimental schemes based on quantum superconducting circuits and inspired by methods used in Josephson parametric

amplification, which should allow one to achieve these driven dissipative processes along with the Hamiltonians ensuring the universal operations in an efficient manner.

Keywords: quantum superconducting circuits, circuit quantum electrodynamics, quantum error correction, quantum reservoir engineering, universal quantum computation

1. Introduction

In a recent paper [1], we showed that a quantum harmonic oscillator could be used as a powerful resource to encode and protect quantum information. In contrast to the usual approach of multi-qubit quantum error correcting codes [2, 3], our approach takes advantage of the infinite dimensional Hilbert space of a quantum harmonic oscillator by redundantly encoding quantum information without the introduction of additional decay channels. Indeed, the far dominant decay channel for a quantum harmonic oscillator, for instance, a microwave cavity field mode, is photon loss. Hence, we only need one type of error syndrome to identify the photon loss error. In this paper, we aim to extend the proposal of [1] as a hardware-efficient protected quantum memory towards a hardware-efficient protected logical qubit with which we can perform universal quantum computations [4].

Before getting to this extension, we recall the idea behind the proposal of [1]. We start by mapping the qubit state $c_0\ |0\rangle + c_1\ |1\rangle$ into a multi-component superposition of coherent states of the harmonic oscillator $\left|\psi_\alpha^{(0)}\right\rangle = c_0\ |0\rangle_L + c_1\ |1\rangle_L = c_0\ \left|C_\alpha^+\right\rangle + c_1\ \left|C_{i\alpha}^+\right\rangle$, where

$$\left|C_\alpha^\pm\right\rangle = \mathcal{N}\left(|\alpha\rangle \pm |-\alpha\rangle\right), \qquad \left|C_{i\alpha}^\pm\right\rangle = \mathcal{N}\left(|i\alpha\rangle \pm |-i\alpha\rangle\right).$$

Here, $\mathcal{N}\left(\approx 1/\sqrt{2}\right)$ is a normalization factor, and $|\alpha\rangle$ denotes a coherent state of complex amplitude α. By taking α large enough, $|\alpha\rangle$, $|-\alpha\rangle$, $|i\alpha\rangle$ and $|-i\alpha\rangle$ are quasi-orthogonal (note that for $\alpha = 2$ considered in most simulations of this paper, $\left|\langle\alpha\,|i\alpha\rangle\right|^2 < 10^{-3}$). Such an encoding protects the quantum information against photon loss events. In order to see this, let us also define $\left|\psi_\alpha^{(1)}\right\rangle = c_0|C_\alpha^-\rangle + ic_1|C_{i\alpha}^-\rangle$, $\left|\psi_\alpha^{(2)}\right\rangle = c_0|C_\alpha^+\rangle - c_1|C_{i\alpha}^+\rangle$ and $\left|\psi_\alpha^{(3)}\right\rangle = c_0|C_\alpha^-\rangle - ic_1|C_{i\alpha}^-\rangle$. The state $\left|\psi_\alpha^{(n)}\right\rangle$ evolves after a photon loss event to $\mathbf{a}\ \left|\psi_\alpha^{(n)}\right\rangle \Big/ \left\|\mathbf{a}\ \left|\psi_\alpha^{(n)}\right\rangle\right\| = \left|\psi_\alpha^{\left[(n+1)\bmod 4\right]}\right\rangle$, where $\mathbf{a}$ is the harmonic oscillator's annihilation operator. Furthermore, in the absence of jumps during a time interval t, $\left|\psi_\alpha^{(n)}\right\rangle$ deterministically evolves to $\left|\psi_{\alpha e^{-\kappa t/2}}^{(n)}\right\rangle$, where κ is the decay rate of the harmonic oscillator. Now, the parity operator $\Pi = \exp\left(i\pi\mathbf{a}^\dagger\mathbf{a}\right)$ can act as a photon jump indicator. Indeed, we have $\left\langle\psi_\alpha^{(n)}\left|\Pi\right|\psi_\alpha^{(n)}\right\rangle = (-1)^n$ and therefore the measurement of the photon number parity can indicate the occurrence of a photon loss event. While the parity measurements keep track of the photon loss events, the deterministic relaxation of the energy, replacing α by $\alpha e^{-\kappa t/2}$, remains inevitable. To overcome this relaxation of energy, we need to intervene before the coherent states start to overlap in a significant manner to re-pump energy into the codeword.

In [1], applying some tools that were introduced in [5], we illustrated that simply coupling a cavity mode to a single superconducting qubit in the strong dispersive regime [6] provides the required controllability over the cavity mode (modeled as a quantum harmonic oscillator) to perform all the tasks of quantum information encoding, protection and energy re-pumping. The proposed tools exploit the fact that in such a coupling regime, both qubit and cavity frequencies split into well-resolved spectral lines indexed by the number of excitations in the qubit and the cavity. Such a splitting in the frequencies gives the possibility of performing operations controlling the joint qubit-cavity state. For instance, the energy re-pumping into the Schrödinger cat state is performed by decoding back the quantum information onto the physical qubit and re-encoding it on the cavity mode by re-adjusting the number of photons. However, such an invasive control of the state exposes the quantum information to decay channels (such as the T_1 and the T_2 decay processes of the physical qubit) and limits the performance of the protection scheme. Furthermore, if one wanted to use this quantum memory as a protected logical qubit, the application of quantum gates on the encoded information would require the decoding of this information onto the physical qubits, performing the operation, and re-encoding it back to the cavity mode. Once again, by exposing the quantum information to un-protected qubit decay channels, we limit the fidelity of these gates.

In this paper, we aim to exploit an engineered coupling of the storage cavity mode to its environment in order to maintain the energy of the encoded Schrödinger cat state. It is well-known that resonantly driving a damped quantum harmonic oscillator stabilizes a coherent state of the cavity mode field. In particular, the complex amplitude α of this coherent state depends linearly on the complex amplitude of the driving field. In contrast, by coupling a quantum harmonic oscillator to a bath where any energy exchange with the bath happens in pairs of photons, one can drive the quantum harmonic oscillator to the two aforementioned two-component Schrödinger cat states $\left|C_\alpha^+\right\rangle$ and $\left|C_\alpha^-\right\rangle$ [7–11]. In section 2 and appendix A, we will exploit such a two-photon driven dissipative process and extend the results of [7–10] by analytically determining the asymptotic behavior of the system for any initial state. In particular, we will illustrate how such a two-photon process allows us to treat the Schrödinger cat states $\left|C_\alpha^+\right\rangle$ and $\left|C_\alpha^-\right\rangle$ (or equivalently the coherent states $\left|\pm\alpha\right\rangle$) as logical $\left|0\right\rangle$ and $\left|1\right\rangle$ of a qubit which is protected against a photon dephasing error channel. Such a logical qubit, however, is not protected against the dominant single-photon loss channel. Therefore, in the same section, we propose an extension of this two-photon process to a four-photon process for which the Schrödinger cat states $\left|C_\alpha^{(0\mathrm{mod}4)}\right\rangle = \mathcal{N}\left(\left|C_\alpha^+\right\rangle + \left|C_{i\alpha}^+\right\rangle\right)$ and $\left|C_\alpha^{(2\mathrm{mod}4)}\right\rangle = \mathcal{N}\left(\left|C_\alpha^+\right\rangle - \left|C_{i\alpha}^+\right\rangle\right)$ (or equivalently the states $\left|C_\alpha^+\right\rangle$ and $\left|C_{i\alpha}^+\right\rangle$) become a natural choice of logical $\left|0\right\rangle$ and $\left|1\right\rangle$. Thus, we end up with a logical qubit which is protected against photon dephasing errors and for which we can also track and correct errors due to the dominant single-photon loss channel by continuous photon number parity measurements [1]. While this work utilizes a combination of a driven-dissipative process and continuous measurements to engineer and protect a qubit, another recent superconducting circuit proposal [12] utilizes a Hamiltonian-based qubit [13] and protected set of gates. It is interesting to note that both proposals protect their respective qubits from dephasing by engineering the qubit basis states.

In section 3, we present a toolbox to perform universal quantum computation with such protected Schrödinger cat states [14]. Applying specific Hamiltonians that should be easily engineered using methods similar to those in Josephson parametric amplification, and in the presence of the two-

photon or four-photon driven dissipative processes, we can very efficiently perform operations such as arbitrary rotations around the Bloch sphere's x-axis and a two-qubit entangling gate. These schemes can be well understood through quantum Zeno dynamics [15–17] where the strong two-photon or four-photon processes continuously project the evolution onto the degenerate subspace of the logical qubit (also known as a decoherence-free subspace [18]). More precisely, the two-photon (resp. four-photon) process could be considered as a strong measurement of the quantum harmonic oscillator, projecting the system on the space spanned by $\left\{\left|C_\alpha^{\pm}\right\rangle\right\}$ (resp. $\left\{\left|C_\alpha^{k \bmod 4}\right\rangle \middle| k = 0, 1, 2, 3\right\}$). The idea of the quantum Zeno dynamics is then to add a Hamiltonian evolution with a time-scale much slower than the projection rate through the measurement. This will lead to a quasi-unitary evolution within the subspace fixed by the measurement. Furthermore, by increasing the separation of the time-scales between the Hamiltonian evolution and the measurement projection rate, this evolution approaches a real unitary. In order to achieve a full set of universal gates, we then only need to perform a $\pi/2$-rotation around the Bloch sphere's y- or z-axis. This is performed by the Kerr effect, induced when we couple the cavity mode to a nonlinear medium such as a Josephson junction (JJ) [19, 20]. We will illustrate that these gates remain protected against the decay channels of all involved quantum systems and could therefore be employed in a fault-tolerant quantum computation protocol.

Finally, in section 4, we propose a readily realizable experimental scheme to achieve the two-photon driven dissipative process along with Hamiltonians needed for universal logical gates. Indeed, we will illustrate that a simple experimental design based on circuit quantum electrodynamics gives us enough flexibility to engineer all the Hamiltonians and the damping operator that are required for the protocols related to the two-photon process. Focusing on a fixed experimental setup, we will only need to apply different pumping drives of well-chosen but fixed amplitudes and frequencies to achieve these requirements. Moreover, comparing to the experimental scheme proposed in [11] (based on the proposal by [21]) our scheme does not require any symmetries in hardware design: in particular, the frequencies of the modes involved in the hardware could be very different, which helps to achieve an important separation of decay times for the two modes. As supporting indications, similar devices with parameters close to those required in this paper have been recently realized and characterized experimentally [20, 22]. An extension of this experimental scheme to the case of the four-photon driven dissipative process is currently under investigation and we will describe the starting ideas.

2. Driven dissipative multi-photon processes and protected logical qubits

2.1. Two-photon driven dissipative process

Let us consider the harmonic oscillator to be initialized in the vacuum state and let us drive it by an external field in such a way that it can only absorb photons in pairs. Assuming furthermore that the energy decay also only happens in pairs of photons, one easily observes that the photon number parity is conserved. More precisely, we consider the master equation corresponding to a two-photon driven dissipative quantum harmonic oscillator (with $\dot{\rho}$ being the time derivative of ρ)

$$\dot{\rho} = \left[\epsilon_{2\mathrm{ph}}\mathbf{a}^{\dagger 2} - \epsilon_{2\mathrm{ph}}^{*}\mathbf{a}^{2}, \rho\right] + \kappa_{2\mathrm{ph}}\mathcal{D}\left[\mathbf{a}^{2}\right]\rho, \tag{1}$$

where

$$\mathcal{D}[A]\rho = A\rho A^{\dagger} - \frac{1}{2}A^{\dagger}A\rho - \frac{1}{2}\rho A^{\dagger}A.$$

When $\rho(0) = |0\rangle\langle 0|$, one can show that the density matrix ρ converges towards a pure even Schrödinger cat state given by the wavefunction $|C_{\alpha}^{+}\rangle = \mathcal{N}\left(|\alpha\rangle + |-\alpha\rangle\right)$, where $\alpha = \sqrt{2\epsilon_{2\mathrm{ph}}/\kappa_{2\mathrm{ph}}}$ and $\mathcal{N}$ is a normalizing factor. Similarly, if the system is initiated in a state with an odd photon number parity such as the Fock state $|1\rangle\langle 1|$, it converges towards the pure odd Schrödinger cat state $|C_{\alpha}^{-}\rangle = \mathcal{N}\left(|\alpha\rangle - |-\alpha\rangle\right)$. Indeed, the set of steady states of equation (1) is given by the set of density operators defined on the two-dimensional Hilbert space spanned by $\{|\alpha\rangle, |-\alpha\rangle\}$ [10]. For any initial state, the system exponentially converges to this set in infinite time, making the span of $\{|-\alpha\rangle, |\alpha\rangle\}$ the asymptotically stable manifold of the system. However, the asymptotic states in this manifold are not always pure states. One of the results of this paper is to characterize the asymptotic behavior of the above dynamics for any initial state (see appendix A). In particular, initializing the system in a coherent state $\rho(0) = |\beta\rangle\langle\beta|$, it converges to the steady state

$$\rho_{\infty} = c_{++}|C_{\alpha}^{+}\rangle\langle C_{\alpha}^{+}| + c_{--}|C_{\alpha}^{-}\rangle\langle C_{\alpha}^{-}| + c_{+-}|C_{\alpha}^{+}\rangle\langle C_{\alpha}^{-}| + c_{+-}^{*}|C_{\alpha}^{-}\rangle\langle C_{\alpha}^{+}|, \qquad (2)$$

with

$$c_{++} = \frac{1}{2}\left(1 + e^{-2|\beta|^2}\right), \qquad c_{--} = \frac{1}{2}\left(1 - e^{-2|\beta|^2}\right),$$

$$c_{+-} = \frac{i\alpha\beta^{*}e^{-|\beta|^2}}{\sqrt{2\sinh\left(2|\alpha|^2\right)}}\int_{\phi=0}^{\pi} d\phi e^{-i\phi} I_0\left(\left|\alpha^2 - \beta^2 e^{2i\phi}\right|\right),$$

where $I_0(.)$ is the modified Bessel function of the first kind. For large enough $|\beta|$, the populations of the even and odd cat states $|C_{\alpha}^{\pm}\rangle$, c_{++} and c_{--} respectively, equilibrate to one-half. At large enough α (see figure 1, top row), if one initializes with a coherent state away from the vertical axis in phase space, then the system will converge towards one of the two steady coherent states $|\pm\alpha\rangle$ (with the sign depending on whether one initialized to the right or the left of the vertical axis). This suggests that if we choose the states $|C_{\alpha}^{+}\rangle$ and $|C_{\alpha}^{-}\rangle$ as the logical qubit states (see figure 2(a)), the two Bloch vectors $|+_X\rangle \approx |\alpha\rangle$ and $|-_X\rangle \approx |-\alpha\rangle$ are robustly conserved. Therefore, we will deal with a qubit where the phase-flip errors are very efficiently suppressed and the dominant error channel is the bit-flip errors (which could be induced by a single-photon decay process). This could be better understood if we consider the presence of a dephasing error channel for the quantum harmonic oscillator. In the presence ofdephasing with rate κ_{ϕ}, but no single-photon decay (we will discuss this later), the master equation of the driven system is given as follows

$$\dot{\rho} = \left[\epsilon_{2\mathrm{ph}}\mathbf{a}^{\dagger 2} - \epsilon_{2\mathrm{ph}}^{*}\mathbf{a}^{2}, \rho\right] + \kappa_{2\mathrm{ph}}\mathcal{D}\left[\mathbf{a}^{2}\right]\rho + \kappa_{\phi}\mathcal{D}\left[\mathbf{a}^{\dagger}\mathbf{a}\right]\rho. \qquad (3)$$

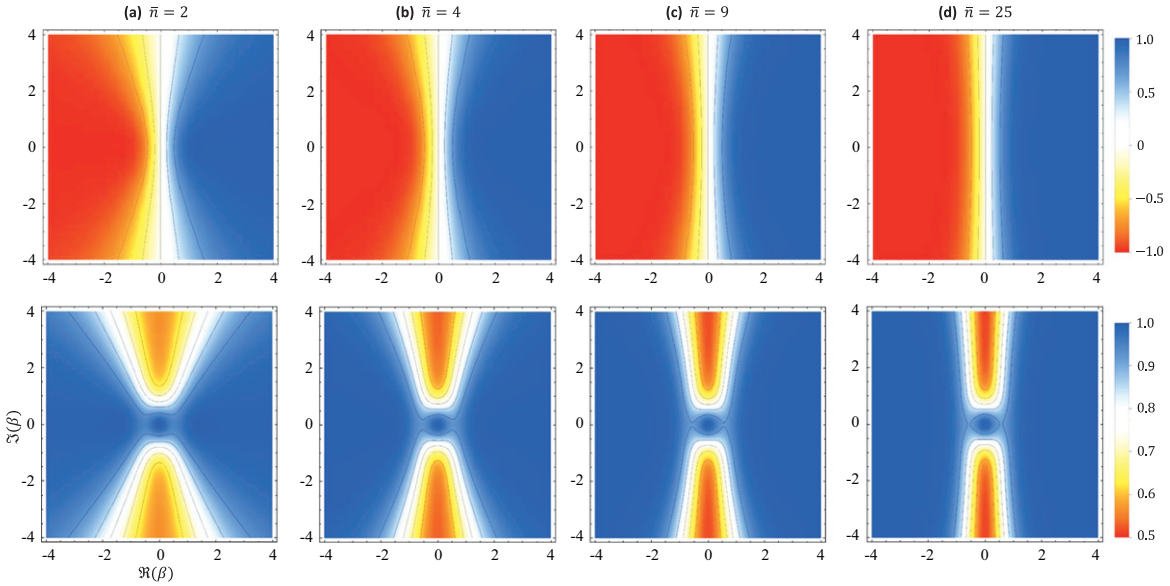

Figure 1. Asymptotic (infinite-time) behavior of the two-photon driven dissipative process given by equation (1) where the density matrix is initialized in a coherent state. Here a point β in the phase space corresponds to the coherent state $|\beta\rangle$ at which the process is initialized. The upper row illustrates the value of the Bloch sphere x-coordinate in the logical basis $\left\{|C_\alpha^+\rangle, |C_\alpha^-\rangle\right\}$ $\left(\approx \langle\alpha| \rho_s |\alpha\rangle - \langle -\alpha| \rho_s |-\alpha\rangle\right)$ where $\alpha = \sqrt{\bar{n}} = \sqrt{2\epsilon_{2\text{ph}}/\kappa_{2\text{ph}}}$ for $\bar{n} = 2$, 4, 9 and 25. We observe that for most coherent states except for a narrow vertical region in the center of the phase space, the system converges to one of the steady coherent states $|\pm\alpha\rangle$. The lower row illustrates the purity of the steady state to which we converge $\left(\text{tr}\left\{\rho_\infty^2\right\}\right)$ for various initial coherent states. Besides the asymptotic state being the pure $|\pm\alpha\rangle$ away from the vertical axis, one can observe that the asymptotic state is also pure for initial states near the center of phase space. Indeed, starting in the vacuum state, the two-photon process drives the system to the pure Schrödinger cat state $|C_\alpha^+\rangle$.

Such a dephasing, similar to the photon drive and dissipation, does not affect the photon number parity. Therefore the populations of the cat states $|C_\alpha^+\rangle$ and $|C_\alpha^-\rangle$, or equivalently the $|+_Z\rangle$ and $|-_Z\rangle$ states in the logical basis, remain constant in the presence of such dephasing. This means that such an error channel does not induce any bit flip errors on the logical qubit. It can however induce phase flip errors. But as shown in appendix A, the rate at which such logical phase flip errors happen is exponentially suppressed by the size of the cat. Indeed, for $\kappa_\phi \ll \kappa_{2\text{ph}}$, the induced logical phase flip rate is given by

$$\gamma_{\text{phase-flip}} \approx \kappa_\phi \frac{|\alpha|^2}{\sinh\left(2|\alpha|^2\right)} \to 0 \quad \text{as} \quad |\alpha| \to \infty.$$

The two-photon driven dissipative process therefore leads to a logical qubit basis which is very efficiently protected against the harmonic oscillator's dephasing channel. It is, however, well known that the major decay channel in usual practical quantum harmonic oscillators is single-

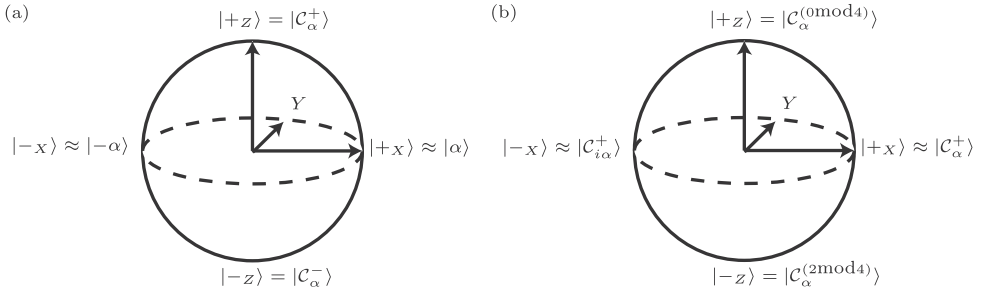

Figure 2. (a) The two-photon driven dissipative process leads to the choice of even and odd Schrödinger cat states $\left|C_\alpha^+\right\rangle$ and $\left|C_\alpha^-\right\rangle$ as the logical $\left|0\right\rangle$ and $\left|1\right\rangle$ of a qubit not protected against the single-photon loss channel. In this encoding, the $\left|+_X\right\rangle$ and $\left|-_X\right\rangle$ Bloch vectors approximately correspond to the coherent states $\left|\alpha\right\rangle$ and $\left|-\alpha\right\rangle$ (the approximate correspondence is due to the non-orthogonality of the two coherent states which is suppressed exponentially by $4|\alpha|^2$. While the coherent states are quasi-orthogonal, the cat states are orthogonal for all values of α. Since the overlap between coherent states decreases exponentially with $|\alpha|^2$, the two sets of states can be considered as approximately mutually unbiased bases for an effective qubit for $|\alpha| \gtrsim 2$). (b) The four-photon driven dissipative process leads to the choice of four-component Schrödinger cat states $\left|C_\alpha^{(0\mathrm{mod}4)}\right\rangle$ and $\left|C_\alpha^{(2\mathrm{mod}4)}\right\rangle$ as the logical $\left|0\right\rangle$ and $\left|1\right\rangle$ of a qubit which can be protected against single-photon loss channel by continuous photon number parity measurements. Here $\left|C_\alpha^{(0\mathrm{mod}4)}\right\rangle = \mathcal{N}\left(\left|C_\alpha^+\right\rangle + \left|C_{i\alpha}^+\right\rangle\right)$ corresponds to a 4-cat state which in the Fock basis is only composed of photon number states that are multiples of four. Similarly $\left|C_\alpha^{(2\mathrm{mod}4)}\right\rangle = \mathcal{N}\left(\left|C_\alpha^+\right\rangle - \left|C_{i\alpha}^+\right\rangle\right)$ corresponds to a 4-cat state which in the Fock basis is composed of states whose photon numbers are the even integers not multiples of 4. In this encoding, $\left|+_X\right\rangle$ and $\left|-_X\right\rangle$ Bloch vectors approximately correspond to the two-component Schrödinger cat states $\left|C_\alpha^+\right\rangle$ and $\left|C_\alpha^-\right\rangle$.

photon loss [23]. While the two-photon process fixes the manifold spanned by the states $\left|C_\alpha^\pm\right\rangle$ as the steady state manifold, the single-photon jumps, that can be modeled by application at a random time of the annihilation operator $\mathbf{a}$, lead to a bit-flip error channel on this logical qubit basis. Indeed, the application of $\mathbf{a}$ on $\left|C_\alpha^\pm\right\rangle$ sends that state to $\left|C_\alpha^\mp\right\rangle$. Such jumps are not suppressed by the two-photon process and a single-photon decay rate of $\kappa_{1\mathrm{ph}}$ leads to a logical qubit bit-flip rate of $|\alpha|^2\kappa_{1\mathrm{ph}}$. It is precisely for this reason that we need to get back to the protocol of [1] recalled in section 1.

2.2. Four-photon driven dissipative process

In order to be able to track single-photon jump events, we need to replace the logical qubit states $\left|C_\alpha^\pm\right\rangle$ by the Schrödinger cat states $\left|C_\alpha^{(0\mathrm{mod}4)}\right\rangle$ and $\left|C_\alpha^{(2\mathrm{mod}4)}\right\rangle$. To this aim, we present here an extension of the above two-photon process to a four-photon one. Indeed, coupling a quantum harmonic oscillator to a driven bath in such a way that any exchange of energy with the bath happens through quadruples of photons obtains the following master equation:

$$\dot{\rho} = \left[\epsilon_{4\mathrm{ph}}\mathbf{a}^{\dagger 4} - \epsilon_{4\mathrm{ph}}^{*}\mathbf{a}^{4}, \rho\right] + \kappa_{4\mathrm{ph}}\mathcal{D}\left[\mathbf{a}^{4}\right]\rho. \tag{4}$$

The steady states of these dynamics are given by the set of density operators defined on the four-dimensional Hilbert space spanned by $\left\{\left|\pm\alpha\right\rangle, \left|\pm i\alpha\right\rangle\right\}$, where $\alpha = \left(2\epsilon_{4\mathrm{ph}}/\kappa_{4\mathrm{ph}}\right)^{1/4}$. In particular, noting that the above master equation conserves the number of photons modulo 4, starting at initial Fock states $\left|0\right\rangle, \left|1\right\rangle, \left|2\right\rangle$ and $\left|3\right\rangle$, the system converges, respectively, to the pure states

$$\begin{aligned} C_{\alpha}^{(0\,\mathrm{mod}\,4)} &= \mathcal{N}\left(\left|C_{\alpha}^{+}\right\rangle + \left|C_{i\alpha}^{+}\right\rangle\right), \quad C_{\alpha}^{(1\,\mathrm{mod}\,4)} = \mathcal{N}\left(\left|C_{\alpha}^{-}\right\rangle - i\,\left|C_{i\alpha}^{-}\right\rangle\right), \\ C_{\alpha}^{(2\,\mathrm{mod}\,4)} &= \mathcal{N}\left(\left|C_{\alpha}^{+}\right\rangle - \left|C_{i\alpha}^{+}\right\rangle\right), \quad C_{\alpha}^{(3\,\mathrm{mod}\,4)} = \mathcal{N}\left(\left|C_{\alpha}^{-}\right\rangle + i\,\left|C_{i\alpha}^{-}\right\rangle\right). \end{aligned}$$

By keeping track of the photon number parity, we can restrict the dynamics to the even parity states, so that the steady states are given by the set of density operators defined on the Hilbert space spanned by $\left\{\left|C_{\alpha}^{(0\ \mathrm{mod}\ 4)}\right\rangle, \left|C_{\alpha}^{(2\mathrm{mod}4)}\right\rangle\right\}$. Similar to the two-photon process, these two states will be considered as the logical, now also protected, $\left|0\right\rangle$ and $\left|1\right\rangle$ of a qubit (see figure 2(b)). Once again, a photon dephasing channel of rate κ_{ϕ} leads to a phase-flip error channel for the logical qubit where the error rate is exponentially suppressed by the size of the Schrödinger cat state (see numerical simulations in appendix A).

Note that probing the photon number parity of a quantum harmonic oscillator in a quantum non-demolition manner can be performed by a Ramsey-type experiment where the cavity mode is dispersively coupled to a single qubit playing the role of the meter [24]. Such an efficient continuous monitoring of the photon number parity has recently been achieved using a transmon qubit coupled to a 3D cavity mode in the strong dispersive regime [25]. Furthermore, we have determined that this photon number parity measurement can be performed in a fault-tolerant manner; the encoded state can remain intact in the presence of various decay channels of the meter. The details of such a fault-tolerant parity measurement method will be addressed in a future publication [26].

3. Universal gates and fault-tolerance

The proposal of the previous section together with the implementation scheme of the next one should lead to a technically realizable protected quantum memory. Having discussed how one can dynamically protect from both bit-flip and phase-flip errors, we show in this section that such a protection scheme can be further explored towards a new paradigm for performing fault-tolerant quantum computation. Having this in mind, we will show how a set of universal quantum gates can be efficiently implemented on such dynamically protected qubits. This set consists of arbitrary rotations around the x-axis of a single qubit, a single-qubit $\pi/2$ rotation around the z-axis, and a two-qubit entangling gate.

The arbitrary rotations around x-axis of a single qubit and the two-qubit entangling gate can be generated by applying some fixed-amplitude driving fields at well-chosen frequencies, leading to additional terms in the effective Hamiltonian of the pumped regime. In order to complete this set of gates, one then only needs a single-qubit $\pi/2$-rotation around either the y- or z-axes. Here we perform such a rotation around the z-axis by turning off the multi-photon

drives and applying a Kerr effect in the Hamiltonian. Such a Kerr effect is naturally induced in the resonator mode through its coupling to the JJ, providing the nonlinearity needed for the multi-photon process. Finally, we will also discuss the fault-tolerance properties of these gates.

3.1. Quantum Zeno dynamics for arbitrary rotations of a single qubit

Let us start with the case of the two-photon process where the quantum information is not protected against single-photon loss. The parity eigenstates $\left|C_\alpha^+\right\rangle$ and $\left|C_\alpha^-\right\rangle$ are invariant states when the exchange of photons with the environment only happens through pairs of photons. Here, we are interested in performing a rotation of an arbitrary angle θ around the x-axis in this logical basis of $\left\{\left|C_\alpha^+\right\rangle, \left|C_\alpha^-\right\rangle\right\}$:

$$X_\theta = \cos\theta\left(\left|C_\alpha^+\right\rangle\left\langle C_\alpha^+\right| + \left|C_\alpha^-\right\rangle\left\langle C_\alpha^-\right|\right) + i\sin\theta\left(\left|C_\alpha^+\right\rangle\left\langle C_\alpha^-\right| + \left|C_\alpha^-\right\rangle\left\langle C_\alpha^+\right|\right).$$

In other to ensure such a population transfer between the even and odd parity manifolds, one can apply a Hamiltonian ensuring single-photon exchanges with the system. We show that the simplest Hamiltonian that ensures such a transfer of population is a driving field at resonance with the quantum harmonic oscillator. The idea consists of driving the quantum harmonic oscillator at resonance where the phase of the drive is chosen to be out of quadrature with respect to the Wigner fringes of the Schrödinger cat state. Furthermore, the amplitude of the drive is chosen to be much smaller than the two-photon dissipation rate. This can be much better understood when reasoning in a time-discretized manner. Let us assume α to be real and the quantum harmonic oscillator to be initialized in the even parity cat state $\left|C_\alpha^+\right\rangle$. Applying a displacement operator $D\left(i\epsilon\right) = \exp\left(i\epsilon\left(\mathbf{a} + \mathbf{a}^\dagger\right)\right)$ with $\epsilon \ll 1$ brings the state towards

$$D\left(i\epsilon\right)\left|C_\alpha^+\right\rangle = \mathcal{N}\left(e^{-i\epsilon\alpha}\left|-\alpha + i\epsilon\right\rangle + e^{i\epsilon\alpha}\left|\alpha + i\epsilon\right\rangle\right).$$

Following the analysis of the previous section, the two-photon process re-projects this displaced state to the space spanned by $\left\{\left|C_\alpha^+\right\rangle, \left|C_\alpha^-\right\rangle\right\}$ without significantly reducing the coherence term; the states $\left|-\alpha + i\epsilon\right\rangle$ and $\left|\alpha + i\epsilon\right\rangle$ are close to the coherent states $\left|-\alpha\right\rangle$ and $\left|\alpha\right\rangle$. Therefore, the displaced state is approximately projected on the state $\cos\left(\epsilon\alpha\right)\left|C_\alpha^+\right\rangle + i\sin\left(\epsilon\alpha\right)\left|C_\alpha^-\right\rangle$. This is equivalent to applying an arbitrary rotation gate of the form $X_{\epsilon\alpha}$ on the initial cat state $\left|C_\alpha^+\right\rangle$. This protocol can also be understood through quantum Zeno dynamics. The two-photon process can be thought of as a measurement which projects onto the steady-state space spanned by $\left\{\left|C_\alpha^+\right\rangle, \left|C_\alpha^-\right\rangle\right\}$. Continuous performance of such a measurement freezes the dynamics in this space while the weaksingle-photon driving field ensures arbitrary rotations around the x-axis of the logical qubit defined in this basis.

In order to simulate such quantum Zeno dynamics, we consider the effective master equation

$$\dot{\rho} = -i\epsilon_X\left[\mathbf{a} + \mathbf{a}^\dagger, \rho\right] + \epsilon_{2\mathrm{ph}}\left[\mathbf{a}^{\dagger 2} - \mathbf{a}^2, \rho\right] + \kappa_{2\mathrm{ph}}\mathcal{D}\left[\mathbf{a}^2\right]\rho. \tag{5}$$

Letting $\epsilon_{2\mathrm{ph}} = \bar{n}\kappa_{2\mathrm{ph}}/2$ and $\alpha = \sqrt{\bar{n}}$, the above Zeno dynamics will occur in the space spanned by $\left\{\left|C_\alpha^-\right\rangle, \left|C_\alpha^+\right\rangle\right\}$ when $\epsilon_X \ll \kappa_{2\mathrm{ph}}$. By initializing the system in the state $\left|C_\alpha^+\right\rangle$ and letting the system evolve following the above dynamics, we numerically simulate the equivalent of a Rabi

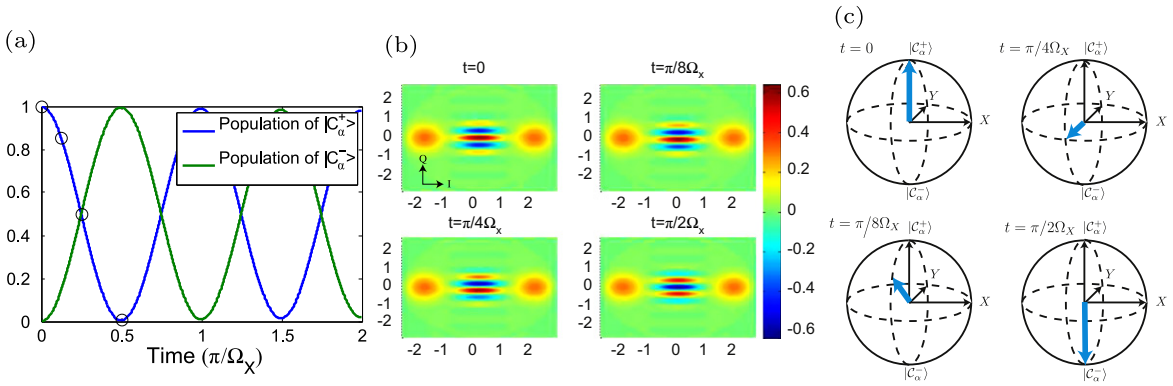

Figure 3. Quantum Zeno dynamics as a tool for performing rotations of an arbitrary angle around the x-axis of the logical qubit space spanned by $\left\{\left|C_\alpha^+\right\rangle, \left|C_\alpha^-\right\rangle\right\}$. The quantum harmonic oscillator is driven at resonance in the Q-direction while the two-photon driven dissipative process is acting on the system. (a) Simulations of equation (5) illustrate the Rabi oscillations around the Bloch sphere's x-axis in the logical qubit space at an effective Rabi frequency of $\Omega_X = 2\epsilon_X\sqrt{\bar{n}}$. Here $\epsilon_X = \kappa_{2\text{ph}}/20$ and $\bar{n} = 4$. (b) Wigner representation of the state at times $t = 0$, $t = \pi/8\Omega_X$, $t = \pi/4\Omega_X$, and $t = \pi/2\Omega_X$. We can observe the shifts in the Wigner fringes while the state remains a coherent superposition with equal weights of $\left|-\alpha\right\rangle$ and $\left|\alpha\right\rangle$. (c) The tomography at these times $t = 0$, $t = \pi/8\Omega_X$, $t = \pi/4\Omega_X$, and $t = \pi/2\Omega_X$ illustrates rotations of angles 0, $\pi/4$, $\pi/2$ and π around the logical x-axis.

oscillation. We monitor the population of the states $\left|C_\alpha^+\right\rangle$ and $\left|C_\alpha^-\right\rangle$ (the $\left|+_Z\right\rangle$ and $\left|-_Z\right\rangle$ states) during the evolution. Figure 3(a) illustrates the result of such simulation over a time of $2\pi/\Omega_X$ where the effective Rabi frequency is given by

$$\Omega_X = 2\epsilon_X\sqrt{\bar{n}}\,.$$

This effective Rabi frequency can be found by projecting the added driving Hamiltonian $\epsilon_X\left(\mathbf{a}+\mathbf{a}^\dagger\right)$ on the space spanned by $\left\{\left|C_\alpha^-\right\rangle, \left|C_\alpha^+\right\rangle\right\}$:

$$\epsilon_X\left(\Pi_{\left|C_\alpha^+\right\rangle}+\Pi_{\left|C_\alpha^-\right\rangle}\right)\left(\mathbf{a}+\mathbf{a}^\dagger\right)\left(\Pi_{\left|C_\alpha^+\right\rangle}+\Pi_{\left|C_\alpha^-\right\rangle}\right) = \left(\alpha+\alpha^*\right)\epsilon_X\left(\left|C_\alpha^+\right\rangle\left\langle C_\alpha^-\right| + \left|C_\alpha^-\right\rangle\left\langle C_\alpha^+\right|\right) = \Omega_X\sigma_x^L,$$

where $\Pi_{\left|C_\alpha^\pm\right\rangle} = \left|C_\alpha^\pm\right\rangle\left\langle C_\alpha^\pm\right|$. One can note in figure 3(a) (where we have chosen $\epsilon_X = \kappa_{2\text{ph}}/20$), the slight decay of the Rabi oscillations as a function of time. This is due to the finite ratio $\kappa_{2\text{ph}}/\epsilon_X$, which adds higher order terms to the above effective dynamics. Indeed, similar computations to the one in appendix A can be performed to calculate the effective dephasing time due to these higher order terms. In practice, this induced decay can be reduced by choosing larger separation of time-scales (smaller $\epsilon_X/\kappa_{2\text{ph}}$) at the expense of longer gate times. However, even a moderate factor of 20 ensures gate fidelities in excess of 99.5%.

As illustrated in figure 3(b), we can calculate the Wigner function at particular times during the evolution. This is performed for the times $t = 0$, $t = \pi/8\Omega_X$, $t = \pi/4\Omega_X$ and

$t = \pi/2\Omega_X$ and, as illustrated in figure 3(c), we observe rotations of angle 0, $\pi/4$, $\pi/2$ and π around the logical x-axis for the qubit states $\left|C_\alpha^+\right\rangle$ and $\left|C_\alpha^-\right\rangle$.

Let us now extend this idea to the case of the four-photon process where quantum information can be protected through continuous parity measurements. For the two-photon process, a population transfer from the even cat state $\left|C_\alpha^+\right\rangle$ to $\left|C_\alpha^-\right\rangle$ is ensured through a resonant drive which provides single-photon exchanges with the system. For the four-photon case, such a rotation of an arbitrary angle around the Bloch sphere's x-axis necessitates a population transfer between the two states $\left|C_\alpha^{0\mathrm{mod}4}\right\rangle$ and $\left|C_\alpha^{2\mathrm{mod}4}\right\rangle$. The state $\left|C_\alpha^{0\mathrm{mod}4}\right\rangle$ corresponds to a four-component Schrödinger cat state, which in the Fock basis is only composed of states with photon numbers that are multiples of 4. Similarly, the state $\left|C_\alpha^{2\mathrm{mod}4}\right\rangle$ corresponds to a four-component Schrödinger cat state which in the Fock basis is only composed of photon number states that are even but not multiples of 4. Therefore, in order to ensure a population transfer from $\left|C_\alpha^{(0\mathrm{mod}4)}\right\rangle$ to $\left|C_\alpha^{(2\mathrm{mod}4)}\right\rangle$, we need to apply a Hamiltonian that adds/subtracts pairs of photons to/from the system. This can be done by adding a squeezing Hamiltonian of the form $\epsilon_X\left(e^{i\phi}a^2 + e^{-i\phi}a^{\dagger 2}\right)$ to the Hamiltonian of the four-photon process (for a real α, we take $\phi = 0$ in order to be in correct quadrature with respect to the Wigner fringes):

$$\dot{\rho} = -i\epsilon_X\left[\mathbf{a}^2 + \mathbf{a}^{\dagger 2}, \rho\right] + \epsilon_{4\mathrm{ph}}\left[\mathbf{a}^{\dagger 4} - \mathbf{a}^4, \rho\right] + \kappa_{4\mathrm{ph}}\mathcal{D}\left[\mathbf{a}^4\right]\rho. \tag{6}$$

In direct correspondence with the two-photon process, we initialize the system in the state $\left|C_\alpha^{(0\mathrm{mod}4)}\right\rangle$ and we simulate equation (6). Here $\epsilon_{4\mathrm{ph}} = \bar{n}^2\kappa_{4\mathrm{ph}}/2$ ensures that the subspace spanned by $\left\{\left|\alpha\right\rangle, \left|-\alpha\right\rangle, \left|i\alpha\right\rangle, \left|-i\alpha\right\rangle\right\}$, with $\alpha = \sqrt{\bar{n}}$, is asymptotically stable. Since all the Hamiltonians and decay terms correspond to exchanges of photons in pairs or quadruples and since we have initialized in $\left|C_\alpha^{0\mathrm{mod}4}\right\rangle$, we can restrict the dynamics to the subspace spanned by even Fock states. In this subspace, the asymptotic manifold is generated by $\left|C_\alpha^{(0\mathrm{mod}4)}\right\rangle$ and $\left|C_\alpha^{(2\mathrm{mod}4)}\right\rangle$. We also take ϵ_X to be much smaller than $\kappa_{4\mathrm{ph}}$. Simulations shown in figure 4(a) (for $\bar{n} = 4$ and $\epsilon_X = \kappa_{4\mathrm{ph}}/20$) illustrate the Rabi oscillations at frequency

$$\Omega_X = 2\epsilon_X\bar{n}$$

around the Bloch sphere's x-axis in this logical basis. This Rabi frequency can also be retrieved by projecting the squeezing Hamiltonian onto the subspace stabilized by the driven dissipative process:

$$\epsilon_X\Pi_{\left|C_\alpha^{(0,1,2,3\mathrm{mod}4)}\right\rangle}\left(\mathbf{a}^2 + \mathbf{a}^{\dagger 2}\right)\Pi_{\left|C_\alpha^{(0,1,2,3\mathrm{mod}4)}\right\rangle} = \left(\alpha^2 + \alpha^{*2}\right)\epsilon_X\left(\sum_{j=0,1,2,3}\left|C_\alpha^{(j\ \mathrm{mod}\ 4)}\right\rangle\left\langle C_\alpha^{(j+2\mathrm{mod}4)}\right|\right).$$

When restricted to the even (or odd) photon number subspace, this precisely gives the effective Hamiltonian $\Omega_X\sigma_x^L$. As shown in figures 4(b), (c), we efficiently achieve an effective single-qubit gate corresponding to rotations of an arbitrary angle around the Bloch sphere's x-axis for the logical qubit spanned by $\left\{\left|C_\alpha^{(0\mathrm{mod}4)}\right\rangle, \left|C_\alpha^{(2\mathrm{mod}4)}\right\rangle\right\}$.

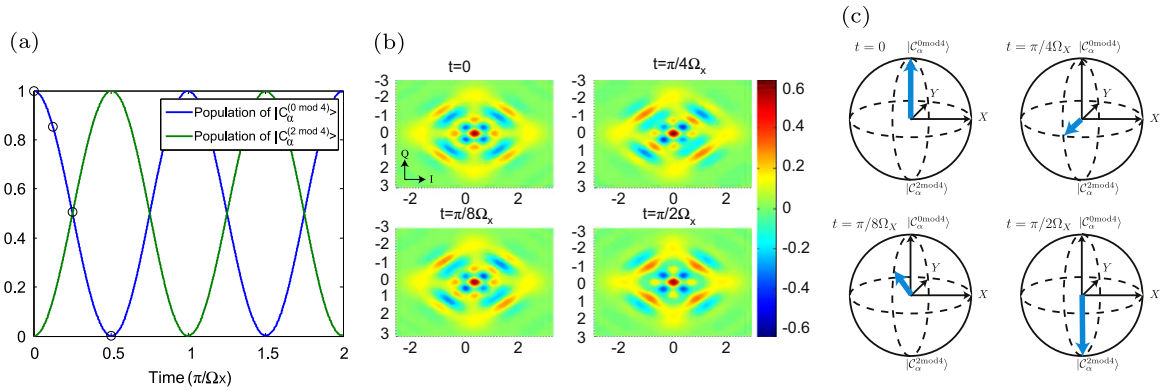

Figure 4. Quantum Zeno dynamics as a tool for performing rotations of arbitrary angles around the Bloch sphere's x-axis of the logical qubit basis of $\left\{\left|C_\alpha^{(0\mathrm{mod}4)}\right\rangle, \left|C_\alpha^{(2\mathrm{mod}4)}\right\rangle\right\}$. A squeezing Hamiltonian is applied on the quantum harmonic oscillator while the four-photon driven dissipative process is acting. (a) Rabi oscillations around the x-axis with an effective Rabi frequency of $\Omega_X = 2\epsilon_X\bar{n}$. Here $\epsilon_X = \kappa_{2\mathrm{ph}}/20$ and $\bar{n} = 4$. (b) Wigner representation of the state at times $t = 0$, $t = \pi/8\Omega_Z$, $t = \pi/4\Omega_Z$ and $t = \pi/2\Omega_Z$, with different fringe patterns associated to rotations with different angles. (c) The tomography at these times $t = 0$, $t = \pi/8\Omega_Z$, $t = \pi/4\Omega_Z$ and $t = \pi/2\Omega_Z$ illustrate rotations of angles 0, $\pi/4$, $\pi/2$ and π around the logical x-axis.

3.2. Quantum Zeno dynamics for a two-qubit entangling gate

Here we show that the same kind of idea can be applied to the case of two logical qubits to produce an effective entangling Hamiltonian of the form $\sigma_x^L \otimes \sigma_x^L$. We start with the case of two harmonic oscillators (with corresponding field mode operators $\mathbf{a}_1$ and $\mathbf{a}_2$), each one undergoing a two-photon process. Let us assume we can effectively couple these two oscillators to achieve a beam-splitter Hamiltonian of the form $\epsilon_{XX}\left(\mathbf{a}_1\mathbf{a}_2^\dagger + \mathbf{a}_2\mathbf{a}_1^\dagger\right)$, where $\epsilon_{XX} \ll \kappa_{1,2\mathrm{ph}}, \kappa_{2,2\mathrm{ph}}$ (we will present in the next section an architecture allowing to get such an effective beam-splitter Hamiltonian between two modes). In order to illustrate the performance of the method, we simulate the two-mode master equation:

$$\begin{aligned}\dot{\rho} &= -i\epsilon_{XX}\left[\mathbf{a}_1\mathbf{a}_2^\dagger + \mathbf{a}_2\mathbf{a}_1^\dagger, \rho\right] + \epsilon_{1,2\mathrm{ph}}\left[\mathbf{a}_1^{\dagger 2} - \mathbf{a}_1^2, \rho\right] + \epsilon_{2,2\mathrm{ph}}\left[\mathbf{a}_2^{\dagger 2} - \mathbf{a}_2^2, \rho\right] \\ &\quad + \kappa_{1,2\mathrm{ph}}\mathcal{D}\left[\mathbf{a}_1^2\right]\rho + \kappa_{2,2\mathrm{ph}}\mathcal{D}\left[\mathbf{a}_2^2\right]\rho. \end{aligned} \tag{7}$$

Simulations in figure 5(a) are performed by initializing the system at the logical state $\left|+_Z, +_Z\right\rangle = \left|C_\alpha^+\right\rangle \otimes \left|C_\alpha^+\right\rangle$ and letting it evolve under equation (7). These simulations illustrate that two-mode entanglement does occur, reaching the Bell states $\left|\mathcal{B}_{2,\alpha}^\pm\right\rangle = \left(\left|C_\alpha^+\right\rangle \otimes \left|C_\alpha^+\right\rangle \pm i\left|C_\alpha^-\right\rangle \otimes \left|C_\alpha^-\right\rangle\right)/\sqrt{2}$. Indeed, by projecting the beam-splitter Hamiltonian $\epsilon_{XX}\left(\mathbf{a}_1\mathbf{a}_2^\dagger + \mathbf{a}_2\mathbf{a}_1^\dagger\right)$ on the tensor product of the spaces spanned by $\left\{\left|C_\alpha^+\right\rangle, \left|C_\alpha^-\right\rangle\right\}$, we obtain the effective Hamiltonian of a two-qubit entangling gate:

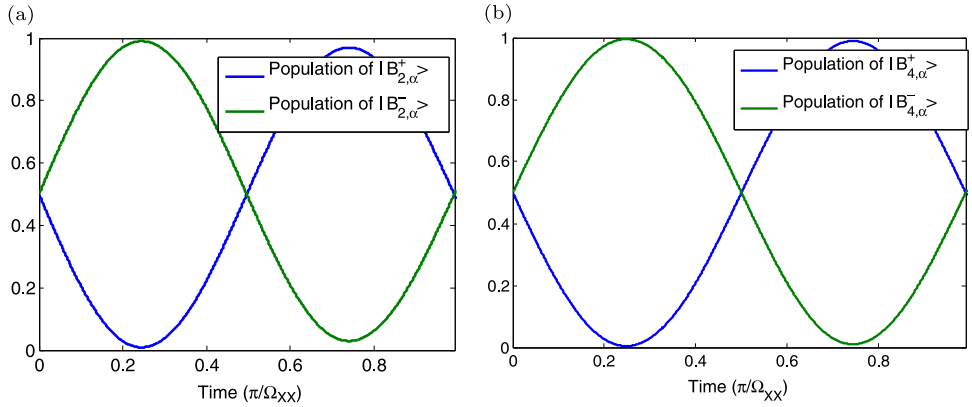

Figure 5. Quantum Zeno dynamics as a tool for performing a two-qubit entangling gate for the two cases of the two-photon process, with the logical qubit basis $\left\{\left|C^+_\alpha\right\rangle, \left|C^-_\alpha\right\rangle\right\}$, and the four-photon process, with the logical qubit basis $\left\{\left|C^{(0\mathrm{mod}4)}_\alpha\right\rangle, \left|C^{(2\mathrm{mod}4)}_\alpha\right\rangle\right\}$. (a) Considering the two-photon process and initializing the effective two-qubit system in the state $\left|+_Z, +_Z\right\rangle = \left|C^+_\alpha\right\rangle \otimes \left|C^+_\alpha\right\rangle$, we monitor continuously the fidelity with respect to the Bell states $\left|\mathcal{B}^\pm_{2,\alpha}\right\rangle = \frac{1}{\sqrt{2}}\left(\left|C^+_\alpha\right\rangle \otimes \left|C^+_\alpha\right\rangle \pm i \left|C^-_\alpha\right\rangle \otimes \left|C^-_\alpha\right\rangle\right)$. The simulation parameters are the same as in previous figures (in particular $\bar{n} = 4$) and the effective entangling Hamiltonian is given by $\Omega_{XX}\sigma_x^{1,L} \otimes \sigma_x^{2,L}$ with $\Omega_{XX} = 2\bar{n}\epsilon_{XX}$ ($\epsilon_{XX} = \kappa_{2\mathrm{ph}}/20$). (b) Similar simulation for the four-photon process, where the effective two-qubit system is initialized in the state $\left|+_Z, +_Z\right\rangle = \left|C^{(0\mathrm{mod}4)}_\alpha\right\rangle \otimes \left|C^{(0\mathrm{mod}4)}_\alpha\right\rangle$ and we monitor continuously the fidelity with respect to the Bell states $\left|\mathcal{B}^\pm_{4,\alpha}\right\rangle = \frac{1}{\sqrt{2}}\left(\left|C^{(0\mathrm{mod}4)}_\alpha\right\rangle \otimes \left|C^{(0\mathrm{mod}4)}_\alpha\right\rangle \pm i \left|C^{(2\mathrm{mod}4)}_\alpha\right\rangle \otimes \left|C^{(2\mathrm{mod}4)}_\alpha\right\rangle\right)$.

$$\epsilon_{XX}\Pi_{\left|C^+_\alpha\right\rangle,\left|C^-_\alpha\right\rangle} \otimes \Pi_{\left|C^+_\alpha\right\rangle,\left|C^-_\alpha\right\rangle}\left(\mathbf{a}_1\mathbf{a}_2^\dagger + \mathbf{a}_2\mathbf{a}_1^\dagger\right)\Pi_{\left|C^+_\alpha\right\rangle,\left|C^-_\alpha\right\rangle} \otimes \Pi_{\left|C^+_\alpha\right\rangle,\left|C^-_\alpha\right\rangle}$$
$$= 2\left|\alpha\right|^2\epsilon_{XX}\left(\left|C^+_\alpha\right\rangle\left\langle C^-_\alpha\right| + \left|C^-_\alpha\right\rangle\left\langle C^+_\alpha\right|\right) \otimes \left(\left|C^+_\alpha\right\rangle\left\langle C^-_\alpha\right| + \left|C^-_\alpha\right\rangle\left\langle C^+_\alpha\right|\right) = \Omega_{XX}\sigma_x^{1,L} \otimes \sigma_x^{2,L},$$

where

$$\Omega_{XX} = 2\bar{n}\epsilon_{XX}.$$

Once again, the decay of the fidelity to the Bell states is due to higher order terms in the above approximation of the beam-splitter Hamiltonian by its projection on the qubit's subspace. This decay can be reduced by taking a larger separation of time-scales between ϵ_{XX} and $\kappa_{1,2\mathrm{ph}}$, $\kappa_{2,2\mathrm{ph}}$. However, as can be seen in the simulations, even with a moderate ratio 1/20 of $\epsilon_{XX}/\kappa_{1,2\mathrm{ph}}$ and $\epsilon_{XX}/\kappa_{2,2\mathrm{ph}}$, we get a Bell state with fidelity in excess of 99%.

For the case of the four-photon process, in order to achieve an effective Hamiltonian of the form $\sigma_x^L \otimes \sigma_x^L$ for the logical qubit basis of $\left\{\left|C^{(0\mathrm{mod}4)}_\alpha\right\rangle, \left|C^{(2\mathrm{mod}4)}_\alpha\right\rangle\right\}$, one needs to ensure exchanges of photons in pairs between the two oscillators encoding the information. This is satisfied by replacing the beam-splitter Hamiltonian with $\epsilon_{XX}\left(\mathbf{a}_1^2\mathbf{a}_2^{\dagger 2} + \mathbf{a}_2^2\mathbf{a}_1^{\dagger 2}\right)$. Once again, we initialize the system in the state $\left|+_Z, +_Z\right\rangle = \left|C^{(0\mathrm{mod}4)}_\alpha\right\rangle \otimes \left|C^{(0\mathrm{mod}4)}_\alpha\right\rangle$ and let it evolve following

the two-mode master equation:

$$\dot{\rho} = -i\epsilon_{XX}\left[\mathbf{a}_1^2\mathbf{a}_2^{\dagger 2} + \mathbf{a}_2^2\mathbf{a}_1^{\dagger 2}, \rho\right] + \epsilon_{1,4\mathrm{ph}}\left[\mathbf{a}_1^{\dagger 4} - \mathbf{a}_1^4, \rho\right] + \epsilon_{2,4\mathrm{ph}}\left[\mathbf{a}_2^{\dagger 4} - \mathbf{a}_2^4, \rho\right] + \kappa_{1,4\mathrm{ph}}\mathcal{D}\left[\mathbf{a}_1^4\right]\rho + \kappa_{2,4\mathrm{ph}}\mathcal{D}\left[\mathbf{a}_2^4\right]\rho. \tag{8}$$

Simulations of figure 5(b) illustrate two-mode entanglement, reaching the Bell states $\left|\mathcal{B}_{4,\alpha}^{\pm}\right\rangle = \left(\left|C_\alpha^{(0\bmod 4)}\right\rangle \otimes \left|C_\alpha^{(0\bmod 4)}\right\rangle \pm i\left|C_\alpha^{(2\bmod 4)}\right\rangle \otimes \left|C_\alpha^{(2\bmod 4)}\right\rangle\right)/\sqrt{2}$. By projecting the Hamiltonian $\epsilon_{XX}\left(\mathbf{a}_1^2\mathbf{a}_2^{\dagger 2} + \mathbf{a}_2^2\mathbf{a}_1^{\dagger 2}\right)$ on the tensor product of the spaces spanned by $\left\{\left|C_\alpha^{(0,1,2,3\bmod 4)}\right\rangle\right\}$ (spaces that are stabilized by the four-photon driven dissipative process), we get the effective Hamiltonian:

$$\epsilon_{XX}\Pi_{\left|C_\alpha^{(0,1,2,3\bmod 4)}\right\rangle} \otimes \Pi_{\left|C_\alpha^{(0,1,2,3\bmod 4)}\right\rangle}\left(\mathbf{a}_1^2\mathbf{a}_2^{\dagger 2} + \mathbf{a}_2^2\mathbf{a}_1^{\dagger 2}\right)\Pi_{\left|C_\alpha^{(0,1,2,3\bmod 4)}\right\rangle} \otimes \Pi_{\left|C_\alpha^{(0,1,2,3\bmod 4)}\right\rangle}$$
$$= 2|\alpha|^4\epsilon_{XX}\left(\sum_{j=0,1,2,3}\left|C_\alpha^{(j \bmod 4)}\right\rangle\left\langle C_\alpha^{(j+2\bmod 4)}\right|\right)^{\otimes 2}.$$

When restricted to the even (or odd) photon number subspace, this gives the two-qubit entangling Hamiltonian $\Omega_{XX}\sigma_x^{1,L} \otimes \sigma_x^{2,L}$, where $\Omega_{XX} = 2\bar{n}^2\epsilon_{XX}$.

3.3. Kerr effect for $\pi/2$-rotation around z-axis

In order to achieve a complete set of universal gates, we only need another single-qubit gate consisting of a $\pi/2$-rotation around the y or z-axis. Together with arbitrary rotations around the x-axis, such a single-qubit gate enables us to perform any unitary operations on single qubits and, along with the two-qubit entangling gate of the previous subsection, provides a complete set of universal gates. However, this fixed angle single-qubit gate presents an issue not manifested in the other gates. To see this, consider the case of the two-photon process with the logical qubit basis $\left\{\left|C_\alpha^+\right\rangle, \left|C_\alpha^-\right\rangle\right\}$. The process renders the two qubit states $\left|\pm_X\right\rangle \approx \left|\pm\alpha\right\rangle$ highly stable and tends to prevent any transfer of population from the vicinity of one of these states to the other one. This is trivially in contradiction with the aim of the $\pi/2$-rotation around the y or z-axis. This simple fact suggests that performing such a gate is not possible in presence of the two-photon process. Here, we propose an alternative approach, consisting of turning off the two-photon process during the operation (possible through the scheme proposed in the next section) and applying a self-Kerr Hamiltonian of the form $-\chi_{\mathrm{Kerr}}\left(\mathbf{a}^\dagger\mathbf{a}\right)^2$. In the next section, we will see how such a Kerr Hamiltonian is naturally produced through the same setting as the one required for the two-photon process.

It was proposed in [19] and experimentally realized in [20] that a Kerr interaction can be used to generate Schrödinger cat states. More precisely, initializing the oscillator in the coherent state $\left|\beta\right\rangle$, at any time $t_q = \pi/q\chi_{\mathrm{Kerr}}$ where q is a positive integer, the state of the oscillator can be written as a superposition of q coherent states [23]:

Table 1. List of Hamiltonians and decay operators providing protection and a set of universal gates

	Two-photon protection	Four-photon protection
Decay operator	$\kappa_{2\mathrm{ph}}\mathbf{a}^2$	$\kappa_{4\mathrm{ph}}\mathbf{a}^4$
Driving Hamiltonian	$i\epsilon_{2\mathrm{ph}}\left(\mathbf{a}^{\dagger 2}-\mathbf{a}^2\right)$	$i\epsilon_{4\mathrm{ph}}\left(\mathbf{a}^{\dagger 4}-\mathbf{a}^4\right)$
Arbitrary rotations around X	$\epsilon_X\left(\mathbf{a}^\dagger+\mathbf{a}\right)$	$\epsilon_X\left(\mathbf{a}^{\dagger 2}+\mathbf{a}^2\right)$
$\pi/2$-rotation around z	$-\chi_{\mathrm{Kerr}}\left(\mathbf{a}^\dagger\mathbf{a}\right)^2$	$-\chi_{\mathrm{Kerr}}\left(\mathbf{a}^\dagger\mathbf{a}\right)^2$
Two-qubit entangling gate	$\epsilon_{XX}\left(\mathbf{a}_1\mathbf{a}_2^\dagger+\mathbf{a}_2\mathbf{a}_1^\dagger\right)$	$\epsilon_{XX}\left(\mathbf{a}_1^2\mathbf{a}_2^{\dagger 2}+\mathbf{a}_2^2\mathbf{a}_1^{\dagger 2}\right)$

$$\left|\psi\left(t_q=\frac{\pi}{q\,\chi_{\mathrm{Kerr}}}\right)\right\rangle=\frac{1}{2q}\sum_{p=0}^{2q-1}\sum_{k=0}^{2q-1}e^{ik\,(k-p)\frac{\pi}{q}}\left|\beta e^{ip\frac{\pi}{q}}\right\rangle.$$

In particular, at $t_2=\pi/2\chi_{\mathrm{Kerr}}$, the states $\left|\pm\alpha\right\rangle$ evolve to $1/\sqrt{2}\left(\left|\pm\alpha\right\rangle-i\left|\mp\alpha\right\rangle\right)$. Therefore, in the case of the logical qubit basis $\left\{\left|C_\alpha^+\right\rangle,\ \left|C_\alpha^-\right\rangle\right\}$, this is equivalent to a $\left(-\pi/2\right)$-rotation around the z-axis.

Analogously for the case of the four-photon process, initializing the oscillator in the two-component Schrödinger cat state $\left|+_X\right\rangle\approx\left|C_\alpha^+\right\rangle$ obtains the state $1/\sqrt{2}\left(\left|C_\alpha^+\right\rangle-i\left|C_{i\alpha}^+\right\rangle\right)$ at time $t_8=\pi/8\chi_{\mathrm{Kerr}}$. Thus, we have a $\left(-\pi/2\right)$-rotation around the z-axis for the logical qubit basis of $\left\{\left|C_\alpha^{(0\bmod 4)}\right\rangle,\ \left|C_\alpha^{(2\bmod 4)}\right\rangle\right\}$.

3.4. Fault-tolerance

The proposed set of Hamiltonians allows one to obtain a set of universal quantum gates for the respective two-photon and four-photon processes (see table 1). In this subsection, we consider a logical qubit encoded by the four-photon driven dissipative process and protected against single-photon decay through continuous photon-number parity measurements. We will discuss the fault-tolerance of the above single and two qubit gates with respect to the decoherence channels of single-photon decay and photon dephasing. Indeed, we will not discuss here the tolerance with respect to imprecisions of the gates themselves as we believe such errors should not be put on the same footing as the errors induced by the decoherence of the involved quantum systems. While the protection against errors due to the coupling to an uncontrolled environment is crucial to ensure a scaling towards many-qubit quantum computation, the degree of perfection of gate parameters, such as the angle of a rotation for instance, can be regarded as a technical and engineering matter.

More precisely, we will prove the first order fault-tolerance of all these quantum operations. Here, by first order fault-tolerance, we mean that we prevent the errors due to single-photon loss or photon dephasing to propagate through various quantum operations (see e.g. definition 4 of [27]). Therefore such an error does not get amplified to produce more errors than can be corrected by the quantum error correction scheme. As we do not address issues such as combining the operations through a concatenation procedure, we do not deal here with a

threshold theorem. In other words, we show that the error rate due to the photon loss channel does not increase while performing the quantum operations of the previous subsections and that the continuous parity measurements during the operations enable the protection against such a decay channel. Furthermore, arbitrary rotations of a qubit around the x-axis as well as the two-qubit entangling gate are performed in presence of the four-photon process, thereby protecting the qubit against photon dephasing. For the single-qubit $\pi/2$-rotation around the z-axis, as long as the Kerr Hamiltonian strength χ_{Kerr} is much more prominent than the dephasing rate (which is the case in most current circuit QED schemes), turning on the four-photon process after the operation will suppress for the phase error accumulated during the operation. Indeed, during the operation, the cavity state is exposed to pure dephasing (rate κ_ϕ) and energy damping (rate $\kappa_{1\text{ph}}$). This gate time is $t_q = \pi/q\chi_{\text{Kerr}}$ ($q = 2$ for the two-photon process and $q = 8$ for the four-photon process). The coherent states forming the encoded quantum state, will have their amplitude reduced by the factor $\exp\left(-\kappa_{1\text{ph}}t_q\right)$, and their phase will drift by a random phase with standard deviation $\delta\varphi = \kappa_\phi t_q$. When the pumping is switched back on at time t_q, these errors will be reduced by a factor which grows exponentially with the cat size, as show in appendix A. Hence these errors can be suppressed in the limit where $\chi_{\text{Kerr}} \gg \kappa_{1\text{ph}}, \kappa_\phi$, and for a sufficiently large α.

Single-qubit X_θ gate and two-qubit entangling gate. These operations would be performed in concurrence with the four-photon process, which continuously and strongly projects to the state space generated by $\left\{\left|\pm\alpha\right\rangle, \left|\pm i\alpha\right\rangle\right\}$. Consider the case of the single-qubit X_θ gate. Starting with the state $\left|+_Z\right\rangle = \left|C_\alpha^{(0\text{mod}4)}\right\rangle$ and in the absence of single-photon jumps, the system evolves at time t to $\left|\psi\left(t\right)\right\rangle = \cos\left(\Omega_X t\right)\ \left|C_\alpha^{(0\text{mod}4)}\right\rangle - i\ \sin\left(\Omega_X t\right)\ \left|C_\alpha^{(2\text{mod}4)}\right\rangle$. With the additional presence of one single-photon jump during this time, this state becomes $\mathbf{a}\left|\psi\left(t\right)\right\rangle = \cos\left(\Omega_X t\right)\ \left|C_\alpha^{(3\text{mod}4)}\right\rangle - i\ \sin\left(\Omega_X t\right)\ \left|C_\alpha^{(1\text{mod}4)}\right\rangle$. Although the qubit has changed basis from the even-parity cat states to their odd-parity counterparts $\left\{\left|C_\alpha^{(3\text{mod}4)}\right\rangle, \left|C_\alpha^{(1\text{mod}4)}\right\rangle\right\}$, the Zeno dynamics ensures that the information preserved in the qubit continues to be rotated by X_θ. After two- and three-photon jumps, we respectively get back to the even and odd parity manifolds, but this time with the order of the basis elements reversed (equivalent to a bit-flip). Finally, after four jumps, we end up in the initial logical basis as if no jump has occurred. This simple reasoning indicates that a continuous photon number parity measurement during the operation should ensure the protection of the rotating quantum information against the single-photon decay channel. The simulations of figure 6 confirm the fact that performing such a single qubit X_θ gate, in the presence of the single-photon decay channel does not increase the decay rate or lead to new decay channels. Continuous photon number parity measurements should therefore correct for such loss events and protect the qubit while the operation is performed. These simulations correspond to the master equation:

$$\dot{\rho} = -i\epsilon_X\left[\mathbf{a}^2 + \mathbf{a}^{\dagger 2}, \rho\right] + \epsilon_{4\text{ph}}\left[\mathbf{a}^{\dagger 4} - \mathbf{a}^4, \rho\right] + \kappa_{4\text{ph}}\mathcal{D}\left[\mathbf{a}^4\right]\rho + \kappa_{1\text{ph}}\mathcal{D}\left[\mathbf{a}\right]\rho.$$

We take $\epsilon_X = 0$ and $\epsilon_X = \kappa_{4\text{ph}}/20$ respectively in figures 6(a) and (b) and $\kappa_{1\text{ph}} = \kappa_{4\text{ph}}/200$ for both plots. As can be seen through these plots, the decay rate remains the same in absence or presence of the two-photon driving field ensuring the arbitrary rotation around the x-axis.

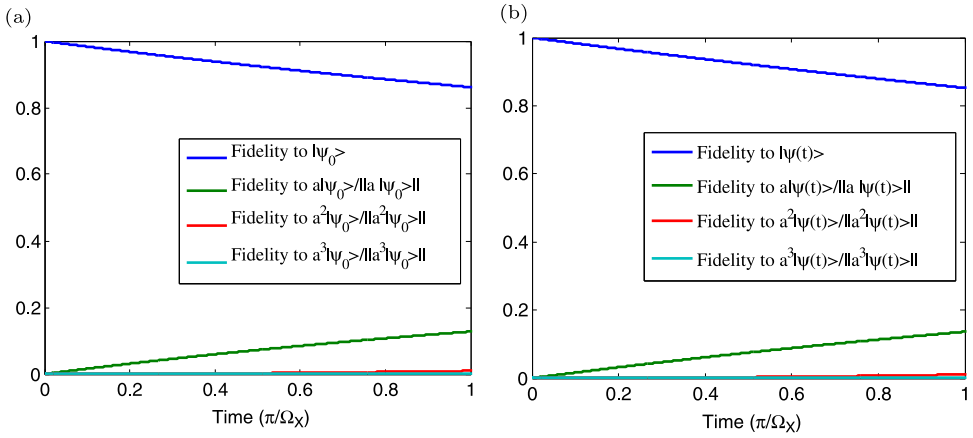

Figure 6. Decay of the unprotected qubit (no photon number parity measurements) encoded in the 4-cat scheme due to single-photon loss channel. (a) The qubit is initialized in the state $\left|\psi_0\right\rangle = \left|C_\alpha^{(0\mathrm{mod}4)}\right\rangle$ and no gate is applied on the qubit ($\bar{n} = 4$ similarly to previous simulations). The decoherence due to the single-photon loss channel leads to a decay in the fidelity with respect to the initial state and creates a mixture of this state with the three other states $\mathbf{a}\left|\psi_0\right\rangle / \left\|\mathbf{a}\left|\psi_0\right\rangle\right\| = \left|C_\alpha^{(3\mathrm{mod}4)}\right\rangle$, $\mathbf{a}^2\left|\psi_0\right\rangle / \left\|\mathbf{a}^2\left|\psi_0\right\rangle\right\| = \left|C_\alpha^{(2\mathrm{mod}4)}\right\rangle$ and $\mathbf{a}^3\left|\psi_0\right\rangle / \left\|\mathbf{a}^3\left|\psi_0\right\rangle\right\| = \left|C_\alpha^{(1\mathrm{mod}4)}\right\rangle$. (b) In the presence of the squeezing Hamiltonian performing the X_θ operation, this decoherence rate remains similar and mixes the desired state $\left|\psi(t)\right\rangle = \cos(\Omega_X t)\left|C_\alpha^{(0\mathrm{mod}4)}\right\rangle - i\sin(\Omega_X t)\left|C_\alpha^{(2\mathrm{mod}4)}\right\rangle$ with the states $\mathbf{a}\left|\psi(t)\right\rangle / \left\|\mathbf{a}\left|\psi(t)\right\rangle\right\| = \cos(\Omega_X t)\left|C_\alpha^{(3\mathrm{mod}4)}\right\rangle - i\sin(\Omega_X t)\left|C_\alpha^{(1\mathrm{mod}4)}\right\rangle$, $\mathbf{a}^2\left|\psi(t)\right\rangle / \left\|\mathbf{a}^2\left|\psi(t)\right\rangle\right\| = \cos(\Omega_X t)\left|C_\alpha^{(2\mathrm{mod}4)}\right\rangle - i\sin(\Omega_X t)\left|C_\alpha^{(0\mathrm{mod}4)}\right\rangle$ and $\mathbf{a}^3\left|\psi(t)\right\rangle / \left\|\mathbf{a}^3\left|\psi(t)\right\rangle\right\| = \cos(\Omega_X t)\left|C_\alpha^{(1\mathrm{mod}4)}\right\rangle - i\sin(\Omega_X t)\left|C_\alpha^{(3\mathrm{mod}4)}\right\rangle$. The photon jumps inducing such mixing of the quantum states are however tractable through continuous photon number parity measurements.

Additionaly, the probability of having more than one jump during the operation time remains within the range of 1%, indicating that with such parameters one would not even need to perform photon-number parity measurements during the operation and that a measurement after the operation would be enough to ensure a significant improvement in the coherence time.

The same kind of analysis is valid for the two-qubit entangling gate. A single-photon loss event for one (or both) of the qubits will lead to switching the associated logical qubit basis of the entangling Hamiltonian $\Omega_{XX}\sigma_x^{1,L} \otimes \sigma_x^{2,L}$, from the even parity manifold to the odd parity one. We can keep track of the encoding subspace for each qubit, by measuring the photon number parity of the two cavity modes after the operation.

Single-qubit $\pi/2$-rotation around z-axis. In order to show that the Kerr effect can be applied in a fault-tolerant manner to perform such a single-qubit operation, we apply some of the arguments of the supplemental material of [1]. We need to consider the effect of photon loss events on the logical qubit during such an operation.

We note first that the unitary generated by the Kerr Hamiltonian does not modify the photon number parity as this Hamiltonian is diagonal in the Fock states basis. Therefore, photon number parity remains a quantum jump indicator in presence of the Kerr effect. Now, let us assume that a jump occurs at time t during the operation: the state after the jump is given by

$$\mathbf{a}e^{it\chi_{Kerr}\left(\mathbf{a}^\dagger\mathbf{a}\right)^2}\left|\psi_0\right\rangle = e^{2it\chi_{Kerr}\mathbf{a}^\dagger\mathbf{a}}e^{it\chi_{Kerr}\left(\mathbf{a}^\dagger\mathbf{a}\right)^2}\mathbf{a}\left|\psi_0\right\rangle,$$

where we have applied the commutation relation $\mathbf{a}f\left(\mathbf{a}^\dagger\mathbf{a}\right) = f\left(\mathbf{a}^\dagger\mathbf{a}+\mathbf{I}\right)\mathbf{a}$, f being an arbitrary analytic function. This means that up to a phase space rotation $e^{i2t\chi_{Kerr}\mathbf{a}^\dagger\mathbf{a}}$, the effect of a photon jump event commutes with the unitary generated by the Kerr Hamiltonian. Assuming much faster parity measurements than the Kerr dynamics and keeping track of both the number of parity jumps p and the times of their occurrences $\left\{t_k\right\}_{k=1}^{p}$, the state after the operation is fully known. In particular, the four-component Schrödinger cat state is rotated in phase space by an angle of $2\left(\sum_{k=1}^{p}t_k\right)\chi_{Kerr}$. We can take this phase space rotation into account by merely changing the phase of the four-photon drive $\epsilon_{4\mathrm{ph}}$ in the four-photon process.

4. Towards an experimental realization within a circuit QED framework

4.1. Two-photon driven dissipative process

In this subsection, we propose an architecture based on Josephson circuits which implements the two-photon driven dissipative process. Using the coupling of cavity modes to a JJ, single-photon dissipation, and coherent drives, we aim to produce effective dynamics in the form of equation (1). These are the same tools used in the Josephson bifurcation amplifier to produce a squeezing Hamiltonian [28] and here we will show that, by selecting a particular pump frequency, we can achieve a two-photon driven dissipative process. Furthermore, in the next subsection, we show that by choosing adequate pump frequencies, we may engineer the interaction terms needed to perform the logical gates described in sections 3.1, 3.2 and 3.3. An architecture suitable for the four-photon driven dissipative process is subject to ongoing work.

The practical device we are considering is represented in figure 7. Two cavities are linked by a small transmission line in which a JJ is embedded. This provides a nonlinear coupling between the modes of these two cavities [20, 22]. The Hamiltonian of this device is given by [29]

$$\mathbf{H}_0 = \sum_k \hbar\omega_k\mathbf{a}_k^\dagger\mathbf{a}_k - E_J\left(\cos\left(\frac{\boldsymbol{\Phi}}{\phi_0}\right)+\frac{1}{2}\left(\frac{\boldsymbol{\Phi}}{\phi_0}\right)^2\right), \qquad \boldsymbol{\Phi} = \sum_k \phi_k\left(\mathbf{a}_k+\mathbf{a}_k^\dagger\right), \quad (9)$$

where E_J is the Josephson energy, $\phi_0 = \hbar/2e$ is the reduced superconducting flux quantum, and ϕ_k is the standard deviation of the zero point flux fluctuation for mode k of frequency ω_k. Here we are only concerned by the dynamics of the fundamental modes of the two cavities and we assume that all other modes are never excited. We denote $\mathbf{a}$ and $\mathbf{b}$ the annihilation operators of these two modes and ω_a, ω_b their respective frequencies. We assume that $|\boldsymbol{\Phi}/\phi_0| \ll 1$ so that we can neglect sixth and higher order terms in the expansion of the cosine. In order to select the terms of interest, we propose to drive mode $\mathbf{b}$ with two fields: a weak resonant drive $\epsilon_b(t)$ and a

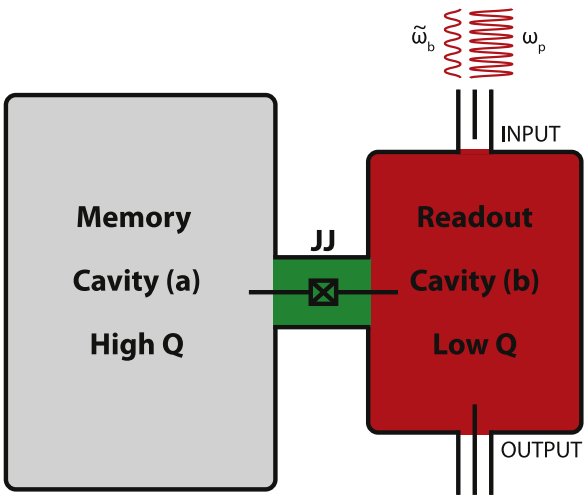

Figure 7. Proposal for a practical realization of the two-photon driven dissipative process. Two cavities are linked by a small transmission line in which a Josephson tunnel junction is embedded. This element provides a nonlinear coupling between the modes of these two cavities. A pump tone at frequency ω_p is applied to the readout cavity. We let **a** and **b** be the annihilation operators for the fundamental modes of the cavities, and $\tilde{\omega}_a$ and $\tilde{\omega}_b$ be their frequencies in the presence of all couplings and the pump. Setting $\omega_p = 2\tilde{\omega}_a - \tilde{\omega}_b$, we select an interaction term of the form $\mathbf{a}^2\mathbf{b}^\dagger$ + c.c. Combining this interaction with a drive and strong single-photon dissipation of mode **b** leads to the desired dynamics for mode **a** of the form equation (1). In this way, quantum information can be stored and protected in mode **a**.

strong off-resonant pump $\epsilon_p(t)$. The frequencies of modes **a** and **b** are shifted by the nonlinear coupling. The dressed frequencies are noted $\tilde{\omega}_a$ and $\tilde{\omega}_b$ and we take $\epsilon_b(t) = 2\epsilon_b \cos(\tilde{\omega}_b t)$ and $\epsilon_p(t) = 2\epsilon_p \cos(\omega_p t)$ with:

$$\omega_p = 2\tilde{\omega}_a - \tilde{\omega}_b.$$

We place ourselves in a regime where rotating terms can be neglected and the remaining terms after the rotating wave approximation constitute the effective Hamiltonian

$$\frac{1}{\hbar}\overline{\mathbf{H}}_{2\mathrm{ph}} = g_{2\mathrm{ph}}\left(\mathbf{a}^2\mathbf{b}^\dagger + \mathbf{a}^{\dagger 2}\mathbf{b}\right) - \epsilon_b\left(\mathbf{b}^\dagger + \mathbf{b}\right) + \frac{\chi_{aa}}{2}\left(\mathbf{a}^\dagger\mathbf{a}\right)^2 + \frac{\chi_{bb}}{2}\left(\mathbf{b}^\dagger\mathbf{b}\right)^2 + \chi_{ab}\left(\mathbf{a}^\dagger\mathbf{a}\right)\left(\mathbf{b}^\dagger\mathbf{b}\right). \quad (10)$$

While the induced self-Kerr and cross-Kerr terms χ_{aa}, χ_{bb} and χ_{ab} can be deduced from the Hamiltonian of equation (9) through the calculations of [29], one similarly finds

$$g_{2\mathrm{ph}} = \frac{\epsilon_p}{\omega_p - \tilde{\omega}_b}\chi_{ab}/2.$$

More precisely, this model reduction can be done by going to a displaced rotating frame in which the Hamiltonian of the pumping drive is removed. Next, one develops the cosine term in the Hamiltonian of equation (9) up to the fourth order and removes the highly oscillating terms in a rotating wave approximation.

Physically, the pump tone ϵ_p allows two-photons of mode **a** to convert to a single-photon of mode **b**, which can decay through the lossy channel coupled to mode **b**. The drive tone ϵ_b

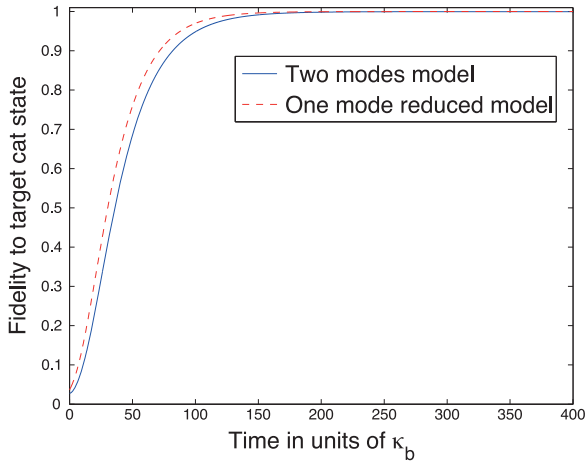

Figure 8. Numerical simulation of equation (11) (full blue line) and equation (1) (dashed red line). We represent the fidelity of the state w.r.t. the state $\left|C_{\alpha}^{+}\right\rangle$, where $\mathcal{N}$ is a normalization factor, and $\alpha = \sqrt{\epsilon_b/g_{2\mathrm{ph}}}$ (here $\bar{n} = |\alpha|^2 = 4$). The dashed and full curves have comparable convergence rates and converge to the same state. This indicates that the reduced model of equation (1) is a faithful representation of the complete model equation (11). The finite discrepancy is due to the finite ratio between $g_{2\mathrm{ph}}$, ϵ_b and κ_b, and the presence of non-zero Kerr and cross-Kerr terms.

inputs energy into mode **b**, which can then be converted to pairs of photon in mode **a**. The last three terms in equation (10) are the Kerr and cross-Kerr couplings inherited from our proposed architecture. Although these are parasitic terms, we show through numerical simulations that their presence does not deteriorate our scheme.

Taking into account single-photon decay of the mode **b**, the effective master equation is given by:

$$\dot{\rho}_{2\mathrm{ph}} = -\frac{i}{\hbar}\left[\overline{\mathbf{H}}_{2\mathrm{ph}}, \rho_{2\mathrm{ph}}\right] + \kappa_b \mathcal{D}[\mathbf{b}]\rho_{2\mathrm{ph}}. \tag{11}$$

Neglecting the Kerr and cross-Kerr terms and assuming that $g_{2\mathrm{ph}}, \epsilon_b \ll \kappa_b$, we adiabatically eliminate mode **b** [7, 30] and find a reduced dynamics for mode **a** of the form of equation (1) where

$$\epsilon_{2\mathrm{ph}} = \frac{2\epsilon_b g_{2\mathrm{ph}}}{\kappa_b}, \quad \kappa_{2\mathrm{ph}} = \frac{4g_{2\mathrm{ph}}^2}{\kappa_b} \text{ and } \alpha = \sqrt{\epsilon_b/g_{2\mathrm{ph}}}.$$

One can check the validity of this model reduction by comparing the numerical simulation of equation (1) to the master equation (11). Fixing $\kappa_b = 1$[4] we take $\chi_{aa} = 0.0015$, $\chi_{bb} = 0.185$, $\chi_{ab} = 0.033$ and $\epsilon_p/\left(\tilde{\omega}_b - \omega_p\right) = 3$, and hence $g_{2\mathrm{ph}} = 0.05$, $\epsilon_b = 4g_{2\mathrm{ph}}$(to fix the average number of photons in the target cat to 4). In figure 8, we compare the fidelity to the target cat state of solutions of equation (11) (blue solid line) and solutions of equation (1), starting

[4] We have intentionally avoided to provide the units to only focus on the separation of time-scales. However, all these parameters will be within the reach of current circuit QED setups if their values are in units of $2\pi \times$ MHz.

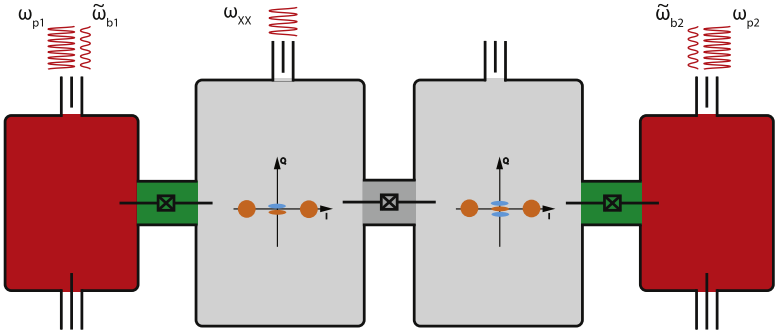

Figure 9. Architecture for coupling two qubits protected by the two-photon driven dissipative processes. Two modules composed of a pair of high and low cavities are connected through a central JJ. This JJ provides a nonlinear coupling between the two storage modes a_1 and a_2 of each module. Adding a pump at frequency $\omega_{XX} = (\tilde{\omega}_{a1} - \tilde{\omega}_{a2})/2$ induces an interaction term of the form $\mathbf{a}_1\mathbf{a}_2^\dagger$ + c.c., thus allowing for the entangling gate detailed in section 3.2

in vacuum. The two curves both converge to a fidelity close to one, which indicates that the steady state of equation (11) is hardly affected by the presence of Kerr and cross-Kerr terms and by the finite ratio of $g_{2\text{ph}}$, ϵ_b to κ_b.

4.2. Logical operations

Rotations of arbitrary angles around the x-axis for the logical qubit $\left\{\left|C_\alpha^+\right\rangle, \left|C_\alpha^-\right\rangle\right\}$: simply adding a drive of amplitude ϵ_a resonant with mode a will add a term proportional to $\epsilon_a^*\mathbf{a} + \epsilon_a\mathbf{a}^\dagger$ in equation (1). In the limit where $\left|\epsilon_a\right| \ll \kappa_{2ph}$, this will induce coherent oscillation between the two states around the Bloch sphere's x-axis, as explained in section 3.1.

Entangling gate between two logical bits: we propose the architecture of figure 9 to couple two qubits protected by a two-photon driven dissipative process. Two modules, each composed of a pair of high and low Q cavities, are coupled through a JJ embedded in a waveguide connecting the two high Q cavities. This JJ provides a nonlinear coupling, which, together with a pump at frequency $\omega_{ZZ} = \left(\tilde{\omega}_{a_1} - \tilde{\omega}_{a_2}\right)/2$, induces an interaction of the form $e^{i\phi_{\text{pump}}}\mathbf{a}_1\mathbf{a}_2^\dagger$ + c.c. Such a term performs an entangling gate between two logical qubits, as described in section 3.2.

$\pi/2$-rotation around z-axis: as mentioned throughout the previous subsection, the mere fact of coupling the cavity mode to a JJ induces a self-Kerr term on the cavity mode. As proposed in section 3.3, this could be employed to perform a $\pi/2$-rotation around the z-axis in a similar manner to [20]. One only needs to turn off all the pumping drives and wait for π/χ_{aa}.

4.3. Extension to four-photon driven dissipative process

Similarly to the case of the two-photon process, we need to achieve an effective Hamiltonian of the form

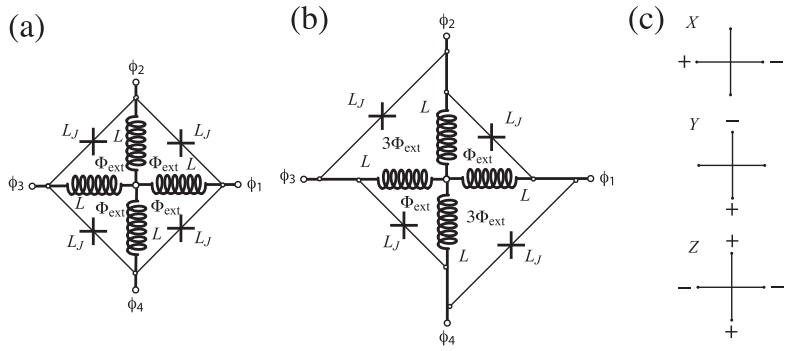

Figure 10. Josephson ring modulators (JRM) providing desired interactions between field modes. (a) JRM developed to ensure quantum limited amplification of a quantum signal or to provide frequency conversion between two modes. The signal and idler are respectively coupled to the X and y modes, as represented in (c) and the pump drive is applied on the z mode. (b) A modification of the amplifier JRM to ensure an interaction of the form of equation (12). Such an interaction should allow us to achieve the driven dissipative four-photon process without adding undesired Hamiltonian terms.

$$\frac{1}{\hbar}\overline{H}_{4\mathrm{ph}} = g_{4\mathrm{ph}}\left(\mathbf{a}^4\mathbf{b}^\dagger + \mathbf{a}^{\dagger 4}\mathbf{b}\right) + \epsilon_b\left(\mathbf{b} + \mathbf{b}^\dagger\right).$$

Taking into account the single-photon decay of the mode **b** of rate κ_b such that $g_{4\mathrm{ph}}$, $\epsilon_b \ll \kappa_b$, we can adiabatically eliminate the mode **b** and find a reduced dynamics for mode **a** of the form of equation (4). The problem is therefore to engineer in an efficient manner the Hamiltonian $\overline{H}_{4\mathrm{ph}}$.

Indeed, the same architecture as in figure 7, together with a pump frequency of $\omega_p = 4\tilde{\omega}_a - \tilde{\omega}_b$, should induce an effective Hamiltonian term of the form $g_{4\mathrm{ph}}\left(\mathbf{a}^4\mathbf{b}^\dagger + \mathbf{a}^{\dagger 4}\mathbf{b}\right)$. One can easily observe this by expanding the cosine term in equation (9) up to the sixth order in $\boldsymbol{\Phi}/\phi_0$ and by applying a rotating wave approximation, leading to an effective coupling strength of $g_{4\mathrm{ph}} = \frac{E_J}{24\hbar}\frac{\epsilon_p}{\omega_p - \tilde{\omega}_b}\frac{\phi_a^4\phi_b^2}{\phi_0^6}$. However, such an architecture also leads to other significant terms limiting the performance of the process. In particular, through the same sixth order expansion, one can observe an amplified induced Kerr effect on the mode **a**: $\chi_{aa}^{\mathrm{pumped}}\left(\mathbf{a}^\dagger\mathbf{a}\right)^2$ with $\chi_{aa}^{\mathrm{pumped}} = \frac{E_J}{4\hbar}\frac{\epsilon_p^2}{\left(\omega_p - \tilde{\omega}_b\right)^2}\frac{\phi_a^4\phi_b^2}{\phi_0^6} = \frac{6\epsilon_p}{\omega_p - \tilde{\omega}_b}g_{4\mathrm{ph}}$.

Inspired by the architecture of the (JRM) [31, 32], which ensures an efficient three-wave mixing, we propose here a design which should induce very efficiently the above effective Hamiltonian while avoiding the addition of extra undesirable interactions. The JRM (figure 10(a)) provides a coupling between the three modes (as presented in figure 10(c)) of the form

$$H_{\rm JRM} = \frac{E_L}{4}\left(\frac{\boldsymbol{\Phi}_X^2}{\phi_0^2}+\frac{\boldsymbol{\Phi}_Y^2}{\phi_0^2}+\frac{\boldsymbol{\Phi}_Z^2}{2\phi_0^2}\right) - 4E_J\left[\cos\frac{\boldsymbol{\Phi}_X}{2\phi_0}\cos\frac{\boldsymbol{\Phi}_Y}{2\phi_0}\cos\frac{\boldsymbol{\Phi}_Z}{2\phi_0}\cos\frac{\Phi_{\rm ext}}{\phi_0}+\sin\frac{\boldsymbol{\Phi}_X}{2\phi_0}\sin\frac{\boldsymbol{\Phi}_Y}{2\phi_0}\sin\frac{\boldsymbol{\Phi}_Z}{2\phi_0}\sin\frac{\Phi_{\rm ext}}{\phi_0}\right],$$

where $E_L=\phi_0^2/L$, $\boldsymbol{\Phi}_{X,Y,Z}=\phi_{X,Y,Z}\left(\mathbf{a}_{X,Y,Z}+\mathbf{a}_{X,Y,Z}^\dagger\right)$, and $\Phi_{\rm ext}/\phi_0$ is the dimensionless external flux threading each of the identical four loops of the device. Furthermore, the three spatial mode amplitudes $\boldsymbol{\Phi}_X=\boldsymbol{\phi}_3-\boldsymbol{\phi}_1$, $\boldsymbol{\Phi}_Y=\boldsymbol{\phi}_4-\boldsymbol{\phi}_2$ and $\boldsymbol{\Phi}_Z=\boldsymbol{\phi}_2+\boldsymbol{\phi}_4-\boldsymbol{\phi}_1-\boldsymbol{\phi}_3$ are gauge invariant orthogonal linear combinations of the superconducting phases of the four nodes of the ring (figure 10(c)).

In the same manner the design of figure 10(b), for a dimensionless external flux of $\Phi_{\rm ext}/\phi_0=\pi/4$ on the small loops and $3\Phi_{\rm ext}/\phi_0=3\pi/4$ on the big loops, induces an effective interaction Hamiltonian of the form

$$H'_{\rm JRM}=\frac{E_L}{4}\left(\frac{\boldsymbol{\Phi}_X^2}{\phi_0^2}+\frac{\boldsymbol{\Phi}_Y^2}{\phi_0^2}+\frac{\boldsymbol{\Phi}_Z^2}{2\phi_0^2}\right)-2\sqrt{2}E_J\sin\frac{\boldsymbol{\Phi}_X}{2\phi_0}\sin\frac{\boldsymbol{\Phi}_Y}{2\phi_0}\left[\sin\frac{\boldsymbol{\Phi}_Z}{2\phi_0}+\cos\frac{\boldsymbol{\Phi}_Z}{2\phi_0}\right]. \tag{12}$$

Similarly to [32], by decreasing the inductances L and therefore increasing the associated E_L, one can keep the three modes of the device stable for such a choice of external fluxes. This however comes at the expense of diluting the nonlinearity.

Now, we couple the z mode of the device to the high-Q storage mode $\mathbf{a}$, its y mode to the low-Q $\mathbf{b}$ mode, and we drive the X mode by a pump of frequency $4\tilde{\omega}_a-\tilde{\omega}_b$ ($\tilde{\omega}_a$ and $\tilde{\omega}_b$ are the effective frequencies of the modes $\mathbf{a}$ and $\mathbf{b}$). By expanding the Hamiltonian of equation (12) up to sixth order terms in $\phi=\left(\frac{\boldsymbol{\Phi}_X}{\phi_0},\frac{\boldsymbol{\Phi}_Y}{\phi_0},\frac{\boldsymbol{\Phi}_Z}{\phi_0}\right)$, the only non-rotating term will be of the form

$$H_{\rm eff}=-\frac{\sqrt{2}}{768}\sqrt{n_{\rm pump}}E_J\frac{\phi_Z^4\phi_Y\phi_X}{\phi_0^6}\left(e^{i\phi_{\rm pump}}\mathbf{a}^4\mathbf{b}^\dagger+e^{-i\phi_{\rm pump}}\mathbf{a}^{\dagger 4}\mathbf{b}\right),$$

where $\phi_{\rm pump}$ is the phase of the pump drive and $n_{\rm pump}$ is the average photon number of the coherent state produced in the pump resonator [33].

5. Summary and conclusions

We have shown that one can achieve a logical qubit basis of cat states $\left\{\left|C_\alpha^+\right\rangle,\left|C_\alpha^-\right\rangle\right\}$ through a two-photon driven dissipative process. A photon dephasing error channel is translated to a phase-flip error rate which is exponentially suppressed by the size $|\alpha|^2$ of the cat states. A single-photon decay channel, however, leads to a bit-flip error channel whose rate is $|\alpha|^2$ times larger than the single-photon decay rate. In order to protect the qubit against such a prominent decay channel, we introduce the similar four-photon driven dissipative process whose logical qubit basis is given by the Schrödinger cat states $\left\{\left|C_\alpha^{(0\bmod 4)}\right\rangle,\left|C_\alpha^{(2\bmod 4)}\right\rangle\right\}$. Once again, the photon dephasing error channel is replaced by a phase-flip error channel whose rate is suppressed exponentially by the size $|\alpha|^2$ of the Schrödinger cat state. A single-photon decay channel leads

to the transfer of quantum information to a new logical basis given by odd Schrödinger cat states $\left\{\left|C_\alpha^{(3\,\mathrm{mod}\,4)}\right\rangle, \left|C_\alpha^{(1\,\mathrm{mod}\,4)}\right\rangle\right\}$. However, we can keep track of single-photon decay by continuously monitoring the photon number parity. Therefore, the cat-state logical qubit can be protected against single-photon decay while also having photon dephasing errors exponentially suppressed.

Next, we have introduced a complete set of universal quantum gates that could be performed on the encoded and protected logical qubits. This set consists of arbitrary rotations around the x-axis of a single qubit, a two-qubit entangling gate, and a single-qubit $\pi/2$ rotation around the z-axis. The first two gates can be performed in presence of the driven dissipative process and through quantum Zeno dynamics. For the last single-qubit gate, we explore the induced Kerr effect of the quantum harmonic oscillator while the driven dissipative process is turned off. We illustrate that these gates can be performed without propagating errors due to photon dephasing or single-photon loss. They have therefore the potential of being integrated in a fault-tolerant quantum computation architecture.

Finally, we have also discussed the implementation of these tools within the framework of circuit quantum electrodynamics. Inspired by methods used in Josephson parametric amplification, we propose simple experimental schemes to achieve, effectively, the multi-photon driven dissipative processes and also various quantum gates introduced through the paper. In particular, we have implemented in our laboratory the system ensuring the two-photon driven dissipative process and the preliminary experimental results are in good agreement with the theory.

Acknowledgments

This research was supported by the Intelligence Advanced Research Projects Activity (IARPA) W911NF-09-1-0369 and by the US Army Research Office W911NF-09-1-0514. MM acknowledges support from the Agence National de Recherche under the project EPOQ2 ANR-09-JCJC-0070. ZL acknowledges support from the NSF DMR 1004406. VVA acknowledges support from the NSF Graduate Research Fellowships Program. LJ acknowledges support from the Alfred P Sloan Foundation, the Packard Foundation, and the DARPA Quiness program.

Appendix A. Asymptotic behavior of the two- and four-photon processes

A.1. Asymptotic state for arbitrary initial state of the two-photon process

As stated in section 2.1, all initial states evolving under the two-photon driven dissipative process from equation (1) will exponentially converge to a specific (possibly mixed) asymptotic density matrix defined on the Hilbert space spanned by the two-component Schrödinger cat states $\left\{\left|C_\alpha^+\right\rangle, \left|C_\alpha^-\right\rangle\right\}$ with $\alpha = |\alpha|e^{i\theta_\alpha}$. In order to characterize the Bloch vector of this asymptotic density matrix ρ_∞ (equation (2)), it is sufficient to determine three degrees of freedom: the population of one of the cats $\left(c_{++} = \left\langle C_\alpha^+\right|\rho_\infty\left|C_\alpha^+\right\rangle\right)$ and the complex coherence between the two $\left(c_{+-} = \left\langle C_\alpha^-\right|\rho_\infty\left|C_\alpha^+\right\rangle\right)$. There exist conserved quantities J_{++}, J_{+-} corresponding to these degrees of

freedom [33] such that $c_{++} = \mathrm{tr}\left\{J_{++}^{\dagger}\rho(0)\right\}$ and $c_{+-} = \mathrm{tr}\left\{J_{+-}^{\dagger}\rho(0)\right\}$ for any initial state $\rho(0)$. These conserved quantities are given by

$$J_{++} = \sum_{n=0}^{\infty} \left|2n\right\rangle\left\langle 2n\right| \tag{A.1}$$

$$J_{+-} = \sqrt{\frac{2|\alpha|^2}{\sinh\left(2|\alpha|^2\right)}} \sum_{q=-\infty}^{\infty} \frac{(-1)^q}{2q+1} I_q\left(|\alpha|^2\right) J_{+-}^{(q)} e^{-i\theta_\alpha(2q+1)}, \tag{A.2}$$

where $I_q(.)$ is the modified Bessel function of the first kind and

$$J_{+-}^{(q)} = \begin{cases} \dfrac{\left(\mathbf{a}^{\dagger}\mathbf{a}-1\right)!!}{\left(\mathbf{a}^{\dagger}\mathbf{a}+2q\right)!!} J_{++}\mathbf{a}^{2q+1} & q \geqslant 0 \\ J_{++}\mathbf{a}^{\dagger 2|q|-1} \dfrac{\left(\mathbf{a}^{\dagger}\mathbf{a}\right)!!}{\left(\mathbf{a}^{\dagger}\mathbf{a}+2|q|-1\right)!!} & q < 0 \end{cases}.$$

In the above, $n!! = n \times (n-2)!!$ is the double factorial. To show that these operators are indeed conserved, first note that an operator J evolves under equation (1) in the Heisenberg picture, i.e.,

$$\dot{J} = \frac{1}{2}\kappa_{2\mathrm{ph}}\left(\left[\alpha^{\star 2}\mathbf{a}^2 - \alpha^2\mathbf{a}^{\dagger 2}, J\right] + 2\mathbf{a}^{\dagger 2}J\mathbf{a}^2 - \mathbf{a}^{\dagger 2}\mathbf{a}^2 J - J\mathbf{a}^{\dagger 2}\mathbf{a}^2\right). \tag{A.3}$$

For the case of equation (A.1), it is easy to see that $\dot{J}_{++} = 0$ since the two-photon system preserves photon number parity and J_{++} is merely the positive parity projector. The off-diagonal quantity from equation (A.2) is an extension of $J_{+-}^{(0)}$, the corresponding conserved quantity for the *non-driven* ($\alpha = 0$) dissipative two-photon process (first calculated in [35]; see also [34]). Each $J_{+-}^{(q)}$ term in the sum for J_{+-} evolves under equation (A.3) as

$$\dot{J}_{+-}^{(q)} = \frac{1}{2}\kappa_{2\mathrm{ph}}(2q+1)\left[\alpha^2 J_{+-}^{(q-1)} - \alpha^{\star 2} J_{+-}^{(q+1)} - 2qJ_{+-}^{(q)}\right].$$

The above equations of motion for $J_{+-}^{(q)}$ mimic the recurrence relation

$$|\alpha|^2\left[I_{q-1}\left(|\alpha|^2\right) - I_{q+1}\left(|\alpha|^2\right)\right] + 2qI_q\left(|\alpha|^2\right) = 0$$

satisfied by the Bessel functions in J_{+-} and both can be used to verify that J_{+-} is indeed conserved. The square root in front of the sum for J_{+-} is chosen such that $\mathrm{tr}\left\{J_{+-}^{\dagger}\left|C_\alpha^+\right\rangle\left\langle C_\alpha^-\right|\right\} = 1$, which can be verified using

$$\left\langle C_\alpha^-\right| J_{+-}^{(q)\dagger}\left|C_\alpha^+\right\rangle = \sqrt{\frac{2|\alpha|^2}{\sinh\left(2|\alpha|^2\right)}} I_q\left(|\alpha|^2\right) e^{i\theta_\alpha(2q+1)} \tag{A.4}$$

as well as the identity (see equation (5.8.6.2) from [36])

$$\sum_{q=-\infty}^{\infty} \frac{(-1)^q}{2q+1} I_q\left(|\alpha|^2\right) I_q\left(|\alpha|^2\right) = \frac{\sinh\left(2|\alpha|^2\right)}{2|\alpha|^2}. \tag{A.5}$$

A.2. Asymptotic state for an initial coherent state of the two-photon process

The conserved quantities $\left\{J_{++}, J_{+-}\right\}$ are sufficient to calculate the population $c_{++} = \left\langle C_\alpha^+\right| \rho_\infty \left|C_\alpha^+\right\rangle$ and coherence $c_{+-} = \left\langle C_\alpha^-\right| \rho_\infty \left|C_\alpha^+\right\rangle$ of the asymptotic state for any initial state $\rho(0)$. Letting $\rho(0) = \left|\beta\right\rangle \left\langle\beta\right|$ with $\beta = |\beta| e^{i\theta_\beta}$, the respective terms are

$$c_{++} = \mathrm{tr}\left\{J_{++}^\dagger \rho(0)\right\} = \frac{1}{2}\left(1 + e^{-2|\beta|^2}\right) \tag{A.6}$$

$$c_{+-} = \mathrm{tr}\left\{J_{+-}^\dagger \rho(0)\right\} = \frac{i\alpha\beta^\star e^{-|\beta|^2}}{\sqrt{2\sinh\left(2|\alpha|^2\right)}} \int_{\phi=0}^{\pi} d\phi e^{-i\phi} I_0\left(\left|\alpha^2 - \beta^2 e^{2i\phi}\right|\right). \tag{A.7}$$

Equation (A.6) is the same simple result as the non-driven case (e.g. equation (3.22) in [32]). To derive equation (A.7), we first apply equation (A.2) to obtain the sum

$$c_{+-} = \frac{\sqrt{2}\,\alpha\beta^\star e^{-|\beta|^2}}{\sqrt{\sinh\left(2|\alpha|^2\right)}} \sum_{q=-\infty}^{\infty} \frac{(-1)^q}{2q+1} I_q\left(|\alpha|^2\right) I_q\left(|\beta|^2\right) e^{i2q\left(\theta_\alpha - \theta_\beta\right)}. \tag{A.8}$$

This sum is convergent because the sum without the $2q+1$ term is an addition theorem for I_q (equation (5.8.7.2) from [34]). To put the above into integral form, we use the identity (derivable from the addition theorem)

$$I_q\left(|\alpha|^2\right) I_q\left(|\beta|^2\right) = \frac{1}{2\pi} \int_{\phi=0}^{2\pi} d\phi e^{iq(\phi+\pi)} I_0\left(\left||\alpha|^2 - |\beta|^2 e^{i\phi}\right|\right).$$

Plugging in the above identity into equation (A.8), interchanging the sum and integral (possible because of convergence), evaluating the sum (which is a simple Fourier series), and performing a change of variables obtains equation (A.7).

When $\alpha = 0$, equation (A.7) reduces to equation (14) from [35]. Assuming real α and using equation (5.8.1.15) from [36], one can calculate limits for large $|\beta|^2$ along the real and imaginary axes in phase space:

$$\begin{aligned} \lim_{\beta\to\infty} c_{+-} &= \frac{1}{2} \frac{\mathrm{erf}\left(\sqrt{2}|\alpha|\right)}{\sqrt{1 - e^{-4|\alpha|^2}}} \xrightarrow{|\alpha|\to\infty} \frac{1}{2} \\ \lim_{\beta\to i\infty} c_{+-} &= -i\frac{1}{2} \frac{\mathrm{erfi}\left(\sqrt{2}|\alpha|\right)}{\sqrt{e^{4|\alpha|^2} - 1}} \xrightarrow{|\alpha|\to\infty} 0 \end{aligned},$$

where $\mathrm{erf}\left(.\right)$ and $\mathrm{erfi}\left(.\right)$ are the error function and imaginary error function, respectively. Both limits analytically corroborate figure 1 and show that the two-photon system is similar to a classical double-well system in the combined large α, β regime.

A.3. Influence of dephasing on the two-photon process

Equation (2) implies that while the states $\left|C_\alpha^{\pm}\right\rangle$ define the basis of our logical qubit, the expectation values of the conserved quantities determine the state of the qubit (or equivalently its Bloch vector). Now let's consider adding the photon dephasing dynamics $\kappa_\phi \mathcal{D}\left[\mathbf{a}^\dagger\mathbf{a}\right]$ to equation (1) and estimate what would happen to the qubit basis elements and more importantly the conserved quantities (determining the effect on the encoded information).

Since dephasing preserves parity, the positive parity projector J_{++} remains conserved and the corresponding population of the cat-state c_{++} thus remains unchanged. The quantity representing the coherence (J_{+-}) to first order decays exponentially at a rate proportional to κ_ϕ. Noting that the population of the states $\left|\pm_Z\right\rangle = \left|C_\alpha^{\pm}\right\rangle$ are conserved, this means that photon dephasing induces only phase-flip errors on our logical qubit. However, this phase-flip rate is itself exponentially suppressed with increasing the number of photons in the cat state $|\alpha|^2$. To see this, we evaluate the first-order perturbative correction due to dephasing on the asymptotic manifold. Since $\left|C_\alpha^{+}\right\rangle\left\langle C_\alpha^{-}\right|$ and J_{+-} are right and left eigenvectors of the super-operator from equation (1) and since dephasing preserves parity, the first order decay rate $\gamma_{\text{phase-flip}}$ is

$$\gamma_{\text{phase-flip}} = -\kappa_\phi \,\text{tr}\left\{J_{+-}^\dagger \mathcal{D}\left[\mathbf{a}^\dagger\mathbf{a}\right]\left|C_\alpha^{+}\right\rangle\left\langle C_\alpha^{-}\right|\right\} = -\kappa_\phi\left\langle C_\alpha^{-}\right|\mathcal{D}\left[\mathbf{a}^\dagger\mathbf{a}\right]J_{+-}^\dagger\left|C_\alpha^{+}\right\rangle.$$

In the above, we have re-arranged for the adjoint of $\mathcal{D}$ to act on J_{+-} instead of $\left|C_\alpha^{+}\right\rangle\left\langle C_\alpha^{-}\right|$ and used $\mathcal{D}^\dagger\left[\mathbf{a}^\dagger\mathbf{a}\right] = \mathcal{D}\left[\mathbf{a}^\dagger\mathbf{a}\right]$ because $\mathbf{a}^\dagger\mathbf{a}$ is Hermitian. Since $J_{+-}^{(q)}$ consist of matrix elements $\left|2n\right\rangle\left\langle 2n+1+2q\right|$ for $n = 0, 1, \ldots$, each term in the sum for J_{+-} has the simple equation of motion

$$\mathcal{D}\left[\mathbf{a}^\dagger\mathbf{a}\right]J\dagger_{+-}(q) = -\frac{1}{2}\kappa_\phi(2q+1)^2 J\dagger_{+-}^{(q)}.$$

The subsequent evaluation of the trace and sum results in the rate

$$\gamma_{\text{phase-flip}} = \kappa_\phi \frac{|\alpha|^2}{\sinh\left(2|\alpha|^2\right)} \tag{A.9}$$

given in section 2.1. We have numerically confirmed (figure A1(a)) that this is indeed the first-order correction to the asymptotic manifold. In the figure, we plot versus $|\alpha|$ the magnitude of the eigenvalue of the evolution operator from equation (3) associated with the decay rate of J_{+-} (which is precisely the phase-flip rate $\gamma_{\text{phase-flip}}$). For small values of $\kappa_\phi/\kappa_{2\text{ph}}$, the numerical result approaches our analytical estimate.

It is worth noting that under the effect of dephasing, the cat-states that comprise the logical qubit basis elements will acquire a small random phase ($\left|C_\alpha^{\pm}\right\rangle$ becomes $\left|C_{\alpha e^{i\phi}}^{\pm}\right\rangle$ where ϕ is a small random phase). Indeed, as an ensemble-averaged result, one can observe that each of the two-dimensional Gaussian peaks that represent the cat state in the phase space slightly smear. However, this smearing merely changes the structure of our qubit basis elements and does not affect the encoded quantum information (represented by J_{++} and J_{+-}).

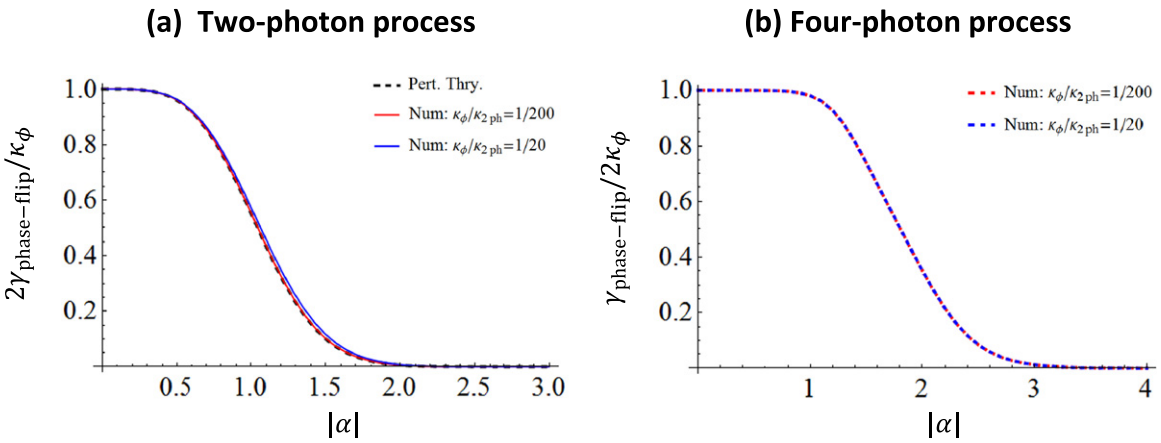

Figure A1. (a) Plot versus $|\alpha|$ of the eigenvalue $\gamma_{\mathrm{phase-flip}}$ (scaled by $\kappa_\phi/2$) of the evolution operator of equation (3) associated with the decay of J_{+-} ($J_{+-}(t) = J_{+-}(0)e^{-\gamma_{\mathrm{phase-flip}}t}$). The plot includes the analytical estimate from equation (A.9) as well as two numerical plots for various $\kappa_\phi/\kappa_{2\mathrm{ph}}$. One can see that the eigenvalue exponentially converges to zero with increasing the photon number in the cat state $|\alpha|^2$. (b) Similar plot for equation (4) with the addition of $\kappa_\phi \mathcal{D}[\mathbf{a}^\dagger\mathbf{a}]$, i.e., the eigenvalue of the evolution operator associated to the decay of J_{02} encoding the coherence term $\left|C_\alpha^{(0 \bmod 4)}\right\rangle\left\langle C_\alpha^{(2 \bmod 4)}\right|$ of the four-photon process qubit. The phase-flip rate is now scaled by $2\kappa_\phi$ which represents the rate for the case of $\alpha = 0$.

A.4. Asymptotic behavior of the four-photon process

The asymptotic manifold of the four-photon process from equation (4) is given by density matrices defined on the four-dimensional Hilbert space spanned by $\left\{\left|C_\alpha^{(\mu \bmod 4)}\right\rangle\right\}$ (with $\mu = 0, 1, 2, 3$). By tracking the parity, we restrict the dynamics to the Hilbert space spanned by $\left\{\left|C_\alpha^{(0 \bmod 4)}\right\rangle, \left|C_\alpha^{(2 \bmod 4)}\right\rangle\right\}$ comprising our logical qubit's basis. The corresponding conserved quantity for the populations of $\left|C_\alpha^{(0 \bmod 4)}\right\rangle$ and $\left|C_\alpha^{(2 \bmod 4)}\right\rangle$ is once again identical to the non-driven case [34], $J_{00} = \sum_{n=0}^{\infty}\left|4n\right\rangle\left\langle 4n\right|$. While an analytical expression for the other conserved quantity J_{02} remains to be found, here we provide a numerical analysis of the influence of the photon dephasing on the four-photon process.

Figure A1(b) shows a plot similar to figure A1(a), but now for $\gamma_{\mathrm{phase-flip}}$ of the logical qubit of the four-photon process. With the exception of a slight delay in the exponential suppression of the induced phase-flip rate, one observes that this suppression is almost identical to the case of the two-photon process.

References

[1] Leghtas Z, Kirchmair G, Vlastakis B, Schoelkopf R J, Devoret M H and Mirrahimi M 2013 Hardware-efficient autonomous quantum memory protection *Phys. Rev. Lett.* **111** 120501

[2] Shor P 1995 Scheme for reducing decoherence in quantum memory *Phys. Rev.* A **52** 2493–6

[3] Steane A 1996 Error correcting codes in quantum theory *Phys. Rev. Lett.* **77** 793–7

[4] Nielsen M A and Chuang I L 2000 *Quantum Computation and Quantum Information* (Cambridge: Cambridge University Press)

[5] Leghtas Z, Kirchmair G, Vlastakis B, Devoret M H, Schoelkopf R J and Mirrahimi M 2013 Deterministic protocol for mapping a qubit to coherent state superpositions in a cavity *Phys. Rev.* A **87** 042315

[6] Schuster D I *et al* 2007 Resolving photon number states in a superconducting circuit *Nature* **445** 515–8

[7] Carmichael H J and Wolinsky M 1988 Quantum noise in the parametric oscillator: from squeezed states to coherent-state superpositions *Phys. Rev. Lett.* **60** 1836–9

[8] Krippner L, Munro W J and Reid M D 1994 Transient macroscopic quantum superposition states in degenerate parametric oscillation: calculations in the large-quantum-noise limit using the positive P representation *Phys. Rev.* A **50** 4330–8

[9] Hach III E and Gerry C C 1994 Generation of mixtures of Schrödinger-cat states from a competitive two-photon process *Phys. Rev.* A **49** 490–8

[10] Gilles L, Garraway B M and Knight P L 1994 Generation of nonclassical light by dissipative two-photon processes *Phys. Rev.* A **49** 2785–99

[11] Everitt M J, Spiller T P, Milburn G J, Wilson R D and Zagoskin A M 2012 Cool for cats arXiv:1212.4795

[12] Brooks P, Kitaev A and Preskill J 2013 Protected gates for superconducting qubits *Phys. Rev.* A **87** 052306

[13] Kitaev A 2006 Protected qubit based on a superconducting current mirror arXiv:/0609441

[14] Gilchrist A, Nemoto K, Munro W J, Ralph T C, Glancy S, Braunstein S L and Milburn G J 2004 Schrödinger cats and their power for quantum information processing *J. Opt. B: Quantum Semiclass. Opt.* **6** S828

[15] Facchi P and Pascazio S 2002 Quantum Zeno subspaces *Phys. Rev. Lett.* **89** 080401

[16] Raimond J-M, Sayrin C, Gleyzes S, Dotsenko I, Brune M, Haroche S, Facchi P and Pascazio S 2010 Phase space tweezers for tailoring cavity fields by quantum Zeno dynamics *Phys. Rev. Lett.* **105** 213601

[17] Raimond J M, Facchi P, Peaudecerf B, Pascazio S, Sayrin C, Dotsenko I, Gleyzes S, Brune M and Haroche S 2012 Quantum Zeno dynamics of a field in a cavity *Phys. Rev.* A **86** 032120

[18] Lidar D A, Chuang I L and Whaley K B 1998 Decoherence-free subspaces for quantum computation *Phys. Rev. Lett.* **81** 2594–7

[19] Yurke B and Stoler D 1986 Generating quantum mechanical superpositions of macroscopically distinguishable states via amplitude dispersion *Phys. Rev. Lett.* **57** 13–16

[20] Kirchmair G, Vlastakis B, Leghtas Z, Nigg S E, Paik H, Ginossar E, Mirrahimi M, Frunzio L, Girvin S M and Schoelkopf R J 2013 Observation of quantum state collapse and revival due to the single-photon Kerr effect *Nature* **495** 205

[21] Kumar S and DiVincenzo D P 2010 Exploiting Kerr cross nonlinearity in circuit quantum electrodynamics for nondemolition measurements *Phys. Rev.* B **82** 014512

[22] Vlastakis B, Kirchmair G, Leghtas Z, Nigg S E, Frunzio L, Girvin S M, Mirrahimi M, Devoret M H and Schoelkopf R J 2013 Deterministically encoding quantum information using 100-photon Schrödinger cat states *Science* **342** 607–10

[23] Haroche S and Raimond J M 2006 *Exploring the Quantum: Atoms, Cavities and Photons* (Oxford: Oxford University Press)

[24] Haroche S, Brune M and M Raimond J 2007 Measuring the photon number parity in a cavity: from light quantum jumps to the tomography of non-classical field states *J. Mod. Opt.* **54** 2101

[25] Sun L *et al* 2013 Tracking photon jumps with repeated quantum non-demolition parity measurements submitted arXiv:1311.2534

[26] Herviou L and Mirrahimi M 2013 Fault-tolerant photon number parity measurement for a quantum harmonic oscillator, in preparation
[27] Gottesman D 2010 An introduction to quantum error correction and fault-tolerant quantum computation *Quantum Information Science and Its Contributions to Mathematics: Proc. Symp. in Applied Mathematics* vol 68 (Providence, RI: American Mathematical Society) pp 13–56 (arXiv:0904.2557)
[28] Vijay R, Devoret M H and Siddiqi I 2009 Invited review article: The Josephson bifurcation amplifier *Rev. Sci. Instrum.* **80** 111101
[29] Nigg S E, Paik H, Vlastakis B, Kirchmair G, Shankar S, Frunzio L, Devoret M H, Schoelkopf R J and Girvin S M 2012 Black-box superconducting circuit quantization *Phys. Rev. Lett.* **108** 240502
[30] Drummond P D, McNeil K J and Walls D F 1981 Non-equilibrium transitions in sub/second harmonic generation II. Quantum theory *Opt. Acta* **28** 211–25
[31] Bergeal N, Vijay R, Manucharyan V E, Siddiqi I, Schoelkopf R J, Girvin S M and Devoret M H 2010 Analog information processing at the quantum limit with a Josephson ring modulator *Nat. Phys.* **6** 296–302
[32] Roch N, Flurin E, Nguyen F, Morfin P, Campagne-Ibarcq P, Devoret M H and Huard B 2012 Widely tunable, non-degenerate three-wave mixing microwave device operating near the quantum limit *Phys. Rev. Lett.* **108** 147701
[33] Schackert F 2013 A practical quantum-limited parametric amplifier based on the Josephson ring modulator *PhD Thesis* Yale University
[34] Albert V V and Jiang L 2014 Symmetries and conserved quantities in Lindblad master equations *Phys. Rev.*A **89** 022118
[35] Simaan H D and Loudon R 1975 Off-diagonal density matrix for single-beam two-photon absorbed light *J. Phys. A: Math. Gen.* **8** 539
[36] Prudnikov A P, Brychkov Y A and Marichev O I 1992 *Integrals and Series Vol 2: Special Functions* 1st edn (London: Gordon and Breach)